Spatial Dynamics and the Mechanoresponse in CD4+ T Cell Activation

Keenan Tali Bashour

Submitted in partial fulfillment of the
requirements for the degree of
Doctor of Philosophy
in the Graduate School of Arts and Sciences

COLUMBIA UNIVERSITY

2013

ABSTRACT

Spatial Dynamics and the Mechanoresponse in CD4+ T Cell Activation

Keenan T. Bashour

The activation of naïve CD4+ T cells by antigen presenting cells is a critical step in the response of the immune system to foreign pathogens and in its acclimation to host tissues. Activation of naïve T cells proceeds through TCR engagement and is further augmented by CD28 costimulation: ensuring T cell survival and conferring numerous functional capabilities. The work in this dissertation highlights the spatial and temporal dynamics that regulate the initial coupling of CD28 with TCR signaling and also dissects the mechanical properties conferred by downstream effectors that are required to relay CD28 costimulation.

A reaction-diffusion model that describes the spatial regulation of costimulation in activating human T cells is developed. The Src kinase Lck, though predominantly cytosolic, is an ideal candidate for the coupling of the TCR and CD28 pathways. Membrane associations bring Lck in contact with these receptors, where mediation of its active state by kinase activity and regulation of its spatial dynamics dictate its capacity to integrate early TCR and CD28 signaling. This developed reaction-diffusion model focusing on Lck is then extrapolated to mouse cells that do not share similar sensitivity to segregation of TCR and CD28 triggering: indicating that while Lck is essential for costimulation, it does not confer spatial sensitivity in activating mouse T cells. A comparison of human and mouse cells demonstrate underlying differences in the

diffusivity of Lck across the membrane and the enrichment of the cytoskeleton at the interface.

The role of the cytoskeleton in generating TCR-driven contractile forces is then investigated through use of micropillar arrays. This approach also enables the quantification of forces generated by T cells during cellular activation. The impact of CD28 costimulation on TCR-driven force generation is assessed and noted to increase cellular forces by 80% beyond what is induced through TCR triggering. By manipulating the presentation of CD28 activation, CD28 is determined to be a mechanoresponsive receptor that is not directly responsible for mechanosensitivty. Rather, CD28 mediates a change in cellular forces through PI3 kinase, whose inhibition normalizes force generation in T cells activated by TCR and those costimulated with TCR and CD28. Downstream of PI3 kinase, PDK1 is identified as being essential in both TCR and CD28 costimulatory force generation; inhibition of PDK1 fully abrogates cellular forces.

Lastly, we qualitatively characterize T cell activation on micropillar arrays, where their complex topology reveals a multiphasic behavior during activation. Whereas T cells activated on planar surfaces are relatively stationary, T cells activated on micropillars slowly migrate towards the base of the array. Forces exerted during this migration are substantially greater than those previously measured, and the slow migration leads to the characterization of multiple phases and the relocalization of key cellular proteins.

Table of Contents Page

I - List of Figures

subsets T_{fh}, T_{H22}, T_{H9} and T-bet+ T_{reg} cells are not mentioned in this discussion, though their unique roles further highlight T cell plasticity.

Figure 1.4. (A) A diagram indicating some of the key players involved in CD4+ T cell activation by an APC. Interactions of note include the TCR-CD3 complex interacting with the MHC class II and the interaction of CD28 with either CD80 or 86. In this diagram, intracellular T cell complexing of these two receptor pairs is mediated Lck, though other Src kinases, including Fyn, are also capable of mediating this interaction. (B) A schematic of the T cell IS. The central SMAC contains activating factors (ie TCR, CD28), the peripheral SMAC contains adhesion factors (ie LFA-1) and distal SMAC is the region where CD45 is excluded to limit its role during T cell activation.

Figure 1.5. Segregation of costimulatory signals. (A) Soft lithography is employed to localization activating antibodies in desired patterns (left column) and result in the distinct localization of the complementary protein (middle and right columns). (B) IL-2 secretion by mouse CD4+ T cells is measured on patterned surfaces at six hours, and demonstrate that colocalization of antibodies targeting CD3 and CD28 [CCO] enhance activation relative to TCR triggering alone [CD3]. Presentation of these antibodies over a wider area further enhance IL-2 secretion, whether these antibodies are segregated by micron scale distances [SEG] or colocalized peripherally [PCO].

Figure 2.1. Spatial Sensitivity to Costimulation. (A) IL-2 is measured at six hours in mouse CD4+ T cells on surfaces that target CD3ε and CD28 in colocalized (coloc) and segregated (seg) patterns. With a background composed of ICAM-1 and BSA (BSA), localizes of CD28 to the periphery of the interface enhances secretion. However, when cholera toxin subunit B (CT-B) is used, secretion of IL-2 is severely curtailed on segregated surfaces. (B) Unlike mouse cells, human T cells show reduced IL-2 secretion at six hours upon segregation of CD3ε and CD28 signaling. The level of IL-2 secretion is comparable to surfaces that do not contain CD28. (C) Staining for active Lck, distinguished by phosphorylation at Tyrosine 393 (pLck), shows differences in mouse and human cells on segregated surfaces. Whereas mouse cells (bottom) show a relatively homogenous distribution, human cells exhibit preferential localization of pLck with sites of TCR activation.

Figure 2.2. Diffusion measurement. (A) FRAP is used to measure the diffusion coefficient in a mouse T cell. The pre-bleach frame shows the distribution of Lck at the surface interface. The subsequent frame shows the result of the subcellular photobleach, approximately 1 μm in diameter. The following frames show the following timelapse. Scale bar denotes 5 μm. (B) Human T cells show reduced mobility relative to mouse cells on homogeneously coated with anti-CD3, anti-CD28 and ICAM-1. Moreover, CT-B impairs the diffusion coefficient of Lck on surfaces. To keep these ligands at a constant concentration between the two conditions, the CT-B fraction was replaced with BSA in the (-) control. (C) The

diffusion of CD4 was measured and showed similar diffusive properties as Lck. CD4 diffusion in human cells was measured at 0.5 ± 0.03 μm^2/sec and 0.26 ± 0.11 μm^2/sec in mouse cells.

Figure 2.3. Cytoskeleton differences in mouse and human lymphocytes. (A) Mouse and human CD4 T cells were stained for phosphorylated Lck [pLck] (red) and F-actin (green) on planar surfaces coated with αCD3, αCD28 and ICAM-1, revealing distinct differences between the two species at 30 minutes. Whereas mouse cells contained enrichment of these two proteins at the periphery of the cell and a moderately diffuse network in the cell center, human cells contain a dense network of both proteins. Treatment of human cells with 1 μm Latrunculin B destabilized the actin cytoskeletal, also manipulating the localization of pLck, which now shows greater colocalization with F-actin. (B) The intensity per unit area of F-actin was greater by a factor of two in human cells than in mouse cells. Treatment of human cells with 1 μm of LatB reduced the average intensity of the actin cytoskeleton. (C) Human cells show a greater interface area, roughly twice the area, than mouse cells. LatB treatment further increases the area of human cells. Together, these quantify the degree of cytoskeletal enrichment at the IS in human cells relative to mouse cells.

Figure 2.4. LatB desensitizes human cells to micropatterns. (A) Treatment of human T cells with LatB increases the lateral diffusion of Lck along the membrane by a factor of 5. (B) Treatment of human T cells with LatB during the first six hours of

activation does not significantly affect IL-2 production on colocalized features. In the absence of LatB, IL-2 secretion on segregated surfaces is comparable to basal activation through CD3 alone. However, LatB treatment substantially increases IL-2 production on segregated patterns, bringing secretion levels on par to those of colocalized features.

Figure 2.5. Latrunculin B modulates localization on micropatterns. (A) Staining for F-actin (green) on segregated patterns of antibodies to CD3ε (red) and CD28 (blue) shows a dense homogeneous distribution in untreated cells (top), whereas LatB treated cells (bottom) show moderate enrichment of F-actin at the site of TCR triggering and a more diffuse network throughout the interface. (B) Staining for active Lck on segregated (left) and colocalized (right, shown in purple) features of CD3ε and CD28 both showed predominant colocalization of active Lck at the site of TCR triggering in untreated cells (top). However, treatment of cells with LatB in both instances resulted in a more even distribution of active Lck along the cell interface.

Figure 3.1. T cells exert forces on micropillar arrays (A) A 2D schematic shows the typical interaction of a T cell (blue) with the antibody-coated micropillar array (red). The displacement due to cellular exertion, δ, is used to calculate the force generated as described in Section 3.2. (B) Four time points that correspond to discrete phases are numbered and shown in (C). In (1), a cell as it first makes contact with the micropillar array. After initial contact, the cell rapidly spreads

(2) while exhibiting minimal contractile force. Cells then initiate force generation on the micropillar array (3) by initially applying unsynchronized contractile forces, marked by white arrows. Finally, cells reach a stable equilibrium (4) where the greatest force exertion occurs along the cell periphery and are oriented towards the center of the cell. Scale bar in C4 denotes 5 μm. (C) A plot of T cell force exertion over time, where each solid trace represents an individual pillar. The blue traces are pillars that are not in contact with the cell, whose ambient movements are tracked and used to remove the contribution of ambient drift from forces generated. The red traces show the interactions of the cell with individual pillars. The dotted cyan line shows the average force exerted on each pillar by the cell, whereas the dotted green line represents the total force exerted by the cell, scaled by 5 so as not to skew the plot. The total force is measured once the net forces have stabilized (here, >1000 seconds).

Figure 3.2. Cellular force exertion across pillar heights. T cell forces were measured across a range of pillar heights, 5-8 μm, that represent a four-fold change in stiffness. Force per area, indicated in black, was found to be consistent across this stiffness range. Likewise, the number of pillars that a cell was in contact with, indicated in red, was also conserved across this stiffness range, indicating that both force per area and total cellular force were conserved. Data is representative of >3 experimental runs. Means are plotted, with error bars representing the standard deviations for both force per area and pillars in contact.

Figure 3.3. Protein enrichment on micropillars. (A) Cytoskeletal constituents F-actin (top, green) and non-muscle Myosin IIA (bottom, green) are stained for in T cells seeded on micropillar arrays. The activating coating, antibodies that activate CD3ε and CD28 (red) is imaged at the interface of the top of the micropillars with the T cell. (B) The active forms of activating factors Zap70 and Lck are stained for. Scale bars denote 5 μm.

Figure 3.4. CD28 activation augments cellular forces. This graph describes the role of CD28 in mediating TCR forces. Inclusion of CD28 activation, either on the coating surface or in solution, equally increases T cell contractile forces. Forces measured here represent the total force exerted by a cell through micropillars. Pillar contact area is not augmented by the inclusion of CD28, either in solution or on the surface, and thus total cell force is proportional to force per area.

Figure 3.5. CD28 modulates cytoskeletal enrichment. (A) Filamin A did not show preferential localization on micropillars when the TCR was triggered (top). However, Filamin A was depleted from micropillars, in a manner similar to Myosin IIA, when CD28 was added to the surface coating (bottom). The relative intensities of pillar surface coating, Filamin A and CD45 are tracked along the white line in the Merged figures, and the distribution of protein is shown on the right. (B) The effect of CD28 activation was measured on Myosin IIA, Filamin A, CD45 and F-actin by Pearson correlation. Whereas Myosin IIA distribution was unaffected by the inclusion of CD28 activation, Filamin A showed a negative

colocalization with the micropillars, indicated by a Pearson value less than 0. Moreover, while CD45 was unperturbed, F-actin showed increased localization to micropillars in the presence of CD28.

Figure 3.6. PI3 Kinase mediates forces through CD28. CD28-dependent contractile forces were tested by selective inhibition of its downstream pathway. PI3 kinases were inhibiting using the more selective wortmannin conjugate 17β-Hydroxywortmannin (HWT), which mitigated the contractile forces generated through CD28 but had no effect on cells activated through CD3 alone. Inhibition of Akt, which is further downstream of PI3 kinase, with Triciribine (Tric) has no effect on cellular force generation. Inhibition of PDK1 with the novel inhibitor GSK 2334470 (GSK) abrogated cellular forces entirely, which is denoted by an asterisk (*).

Figure 4.1. T cell morphology over time. (A) T cells exhibit multiple distinct phases on activating micropillars. The initial contractile behavior where force measurements are taken (left) is later replaced by an intermediate phenotype (middle), where cells extend filopedial projections to interface with the surface. After some time, cells fully relocalize to the base of the array (right):, exhibiting an invasive phenotype. Scalebar represents 5 μm. (B) Tracking cell behavior and classifying them into these three phases over time shows that the majority of cells exit the contractile phase by 8 hours following initial activation. Scale bars denote 5 μm. Temporal tracking fractions are a weighted average of three experiments.

Figure 4.2. Invasive cells are activated. IL-2 measurements from 12 to 13 hours after seeding demonstrate that invasive cells are capable of secreting IL-2. The level of secretion was comparable between micropillars of 1.7 kPa (5μm) and 0.3 kPa (9 μm), though both secreted roughly one half of adjacent cells that spread on regions of planar PDMS (2 MPa stiffness).

Figure 4.3. The position of the MTOC is tracked and found to be coordinated with the movement of the T cell to the base of the array by staining for β-Tubulin (green). In contractile cells (left) the MTOC delays in its movement to the site of activation, and is located in the region between the mid and upper cell. In invasive cells (right) the MTOC relocalizes to the base of the array, and is located between the pillar base and mid pillar. White scale bar denotes 5 μm. Change in Z height from level to level is roughly 3 μm.

Figure 4.4. Protein redistribution in invasive cells. (A) Staining for TCR activation, indicated by phosphorylated Zap70 Y319, shows a relocalization of activating signal to the base of the array. (B) Staining for F-actin cytoskeleton showed distribution along the cell periphery, with substantial enrichment at the points of contact with micropillars. (C) Non-muscle Myosin IIA remains relatively diffuse throughout cells, though is physically segregated from the site of F-actin and CD45 enrichment along the perimeter.

Figure 4.5. TCR activation induces morphological changes. T cells were activated on cellular trenches, where the planar top regions were coated via microcontact printing with either CD3 (left image, blue) or poly-L-lysine (PLL, right image, blue). The base and sides of the trenches were then backfilled with BSA (red) to ensure that any behavior pertaining to the trenches would be motivated by topology rather than protein interactions. Cells that with activated with CD3 ±CD28 extended filopedial protrusions into these trenches, as indicated by an actin stain (green). However, cells that were coated on PLL did not exhibit similar protrusions.

Figure 4.6. Measurement of bmDC forces (A) A representative image of a bmDC generating forces on 5 μm pillars, along with (B) the accompanying brightfield image. (C) Measurement of bmDC forces across pillars of different spring constants demonstrated a behavior similar to T cells, where force generation rather than pillar displacement was consistent.

II - List of Abbreviations

APC	–	Antigen-Presenting Cell
bmDC	–	Bone marrow-derived dendritic cell
BSA	–	Bovine Serum Albumin
CT-B	–	Cholera Toxin subunit B
CTL	–	Cytotoxic T lymphocyte (AKA CD8+ T cell)
FBS	–	Fetal Bovine Serum
FRAP	–	Fluorescence Recovery after Photobleaching
GM1	–	Monosialoganglioside 1
GM-CSF	–	Granulocyte-Macrophage Colony-Stimulating Factor
HWT	–	Wortmannin 17β-hydroxy analog
IL-2	–	Interleukin 2
IS	–	Immune Synapse
LatB	–	Latrunculin B
mTOR	–	Mammalian target of rapamycin
MHC	–	Major histocompatibility complex
PBS	–	Phosphate buffered saline
PI3K	–	Phosphoinositide 3-kinase
RECIST	–	Response Evaluation Criteria in Solid Tumors
SMAC	–	Supramolecular activation cluster
TCR	–	T cell receptor
TIRF	–	Total Internal Reflection Microscopy
WASp	–	Wiskott-Aldrich syndrome protein

III - Acknowledgements

Though one name may be listed on the first page of this thesis, there is no small amount of credit due to a very large number of individuals.

As the most immediate presence involved with this body of work, I would first like to thank Lance for his guidance, creativity, wit and enthusiasm throughout this final stage of my studies. I think how quickly time has flown by is a testament to how well you have done as a PI. To name but a few, the open door policy, effortless aptitude with theoretical concepts and genuine passion for research all have made this a much easier (dare I say pleasant?) road to cross.

As the most immediate presence involved with everything outside this body of work, I would like to thank my parents for their unrequited support and unconditional love (the latter being requited – I'm not callous). Few people have gifted me the freedom and the encouragement to pursue whatever my interests may be. You have raised us to be capable, confidence and independent. I would also like to thank my siblings, Karen and Ryan. I can think of no two other individuals who after I have known for so many years still always manage to leave me in wonder and awe.

I would like to thank the professors and staff in the BME department for their approachability and raw talent. New York is supposed to be an unfriendly city of self-centered egotists; clearly none of you belong here. In particular, I would like to thank my

committee members: Drs Silvia Curado, Henry Hess, Clark Hung, and Gordana Vunjak-Novakovic.

I would also like to say a special thank you to our three former lab members, Peng Shi, Keyue Shen and Jones Tsai, who helped me and Ed get situated in lab while they were also trying to finish their research projects, find jobs and keep their two wives and fiancé happy. A similar thanks to the current members of the lab, Sarah De Leo, Debjit Dutta, Haoqian Chan, Geraldine Hickey, Susie Jin, Edward Judokusumo, Helen Lee and Erdem Tabdanov, for their endearing personalities and daily putting-up-with me. With the lot of you around, I know I can leave the lab in capable and ambitious hands. I would also like to thank the students, both past and present, in the BME department. Having a community that simply does everything and does it all well has been something that you have all taught me to take for granted.

On the technical front, I would like to thank Manus Biggs, Sasha Gondarenko, Jacob Rosenstein, Siddarth Ramakrishnan, Teresa Fazio, Vincent Lee, Ryan Field and Marshall Cox for lending their expertise in microfabrication. I would also like to thank Simon Moore, Pere Roca-Cusachs, Luis Santos and Giovanni Meacci for their expertise in cellular mechanics and signal transduction.

Chapter 1 - Introduction

1.1 Cancer and Immunity

Healthcare costs in the US are growing, both in part to an aging population and also due to the increase in new treatment costs. Cancer accounts for roughly $100 billion in direct costs: second only to the $300 billion cost of cardiovascular disease [CVD] care [1]. The difference is that CVD treatments have been largely successful and has been integral to the increase in overall life expectancy. As the overall death rate and the death rate for CVD decreases year over year, the cancer-associated death rate has remained relatively constant (Figure 1.1). Moreover, cancer is becoming increasingly responsible for mortality in younger generations (Figure 1.1). Cancer prevalence is on the rise, motivating research into new treatment strategies [2].

Though there has been substantial effort and funding for cancer research, the moderate pace of improvement in therapies is not without reason. Cancer is a heterogeneous disease, the complexity of which is well-captured in a pair of articles published in 2000 and 2011 by Douglas Hanahan, where he describes a paradigm of discrete traits that a tumor must acquire in order to be malignant [3, 4]. Together these two articles provide an interesting metric to assess new insights glean from the past decade of cancer research. In the more recent article, Hanahan points to two previously overlooked features of tumor progressions: the proactive reallocation of energy metabolism and the tolerization of immune cells to tumor progression. The latter facet, the attenuation of an immune response, is a feat that few pathogens can sustain for more than a few weeks. The fallout of this revelation has been a number of compelling approaches to reeducate the immune

system. Nascent ambitions to reeducate the immune system stem from the field of vaccination. Approaches to more directly mature the immune system have slowly begun to manifest into its own discipline, encompassing a variety of techniques that are collectively referred to as adoptive immunotherapy.

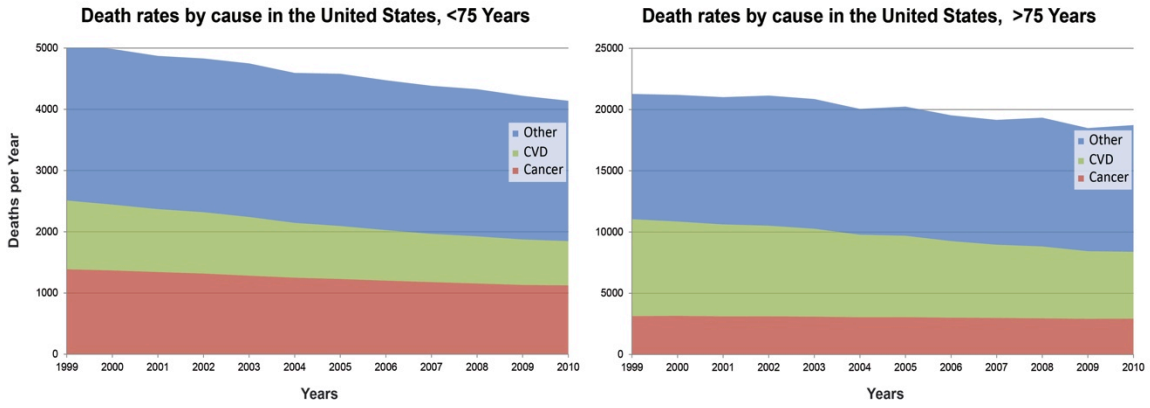

Figure 1.1. Annual **d**eath rates per 100,000 in the United States, from 1999 to 2010. The left graph displays the death rates for those younger than 75 years and the right graph displays the death rates for those over 85 years. Cancer and cardiovascular disease [CVD] are the two most prevalent in the population. Cancer-related deaths are marked in red, those from CVD in green and all others in blue. Whereas the past decade has seen a decline in both overall death rates and CVD-associated deaths, the death rate due to cancer has remained unchanged. Cancer is the most prevalent cause of death in the United States in younger populations, as indicated in the left graph showing the death rate in those under the age of 75. Source of data: CDC

1.2. Adoptive Immunotherapy

The immune system is responsible for detecting and neutralizing pathogens: a task it performs through numerous intermediates. There is, however, the persistent concern of collateral damage to native tissues. The precarious balance of recognizing foreign pathogens while not endangering normal cellular processes manifests in circumstances

where the immune system fails in one of these two primary tasks. A failure in targeting a valid antigen leads to proliferation of undesired cells, whereas an unintended response against native tissue leads to autoimmunity. As a treatment strategy, for potentially both chronic infection and autoimmunity, there has been a hope of harnessing and directly controlling immune cells (Figure 1.2). This process, known as adoptive immunotherapy, was first conceptually validated in 1957 but did not see FDA approval for therapeutic use until 2010 [5]. What 50 years of research and over 100 clinical trials employing adoptive immunotherapy have taught us is that we have only begun to understand the complex process through which an immune response is elicited. The majority of these clinical attempts to reeducate the immune system failed to establish a presence that persisted for a sufficient timescale to be effective, suggesting that while we have identified many of the key cellular and protein players, we have yet to understand the significance of their interactions. To more effectively develop robust and tailored therapies necessitates a mechanistic approach in understanding how an immune response is relayed from one cell to another.

Historically, clinical attempts to harness the immune system have relied on antigen-presenting cells [APC]. These early trials were seen as a recapitulation of an immune response to a vaccine that was executed ex vivo, leading to the early classification as a therapeutic vaccine: one that is delivered in a non-prophylactic manner[1]. Of the APCs, dendritic cells [DC] are the ideal vector, due in large part to their high plasticity, capacity to activate both CD4+ and CD8+ T cells, established markers indicating immature and

[1] With the increase in opportunities and application of vaccine-strategies, these terms have been further refined to include subclasses, such as pre and post exposure prophylactic vaccines, and additional new classes such as adjuvant vaccines.

mature states and their unique ability of cross-presentation. Considerations for adoptive immunotherapy are still multifaceted; current variables include the type of immune cell used to modulate a response, the maturation state of the cell, the method used to isolate and mature cells, the number of cells per transfusion, the route of administration,

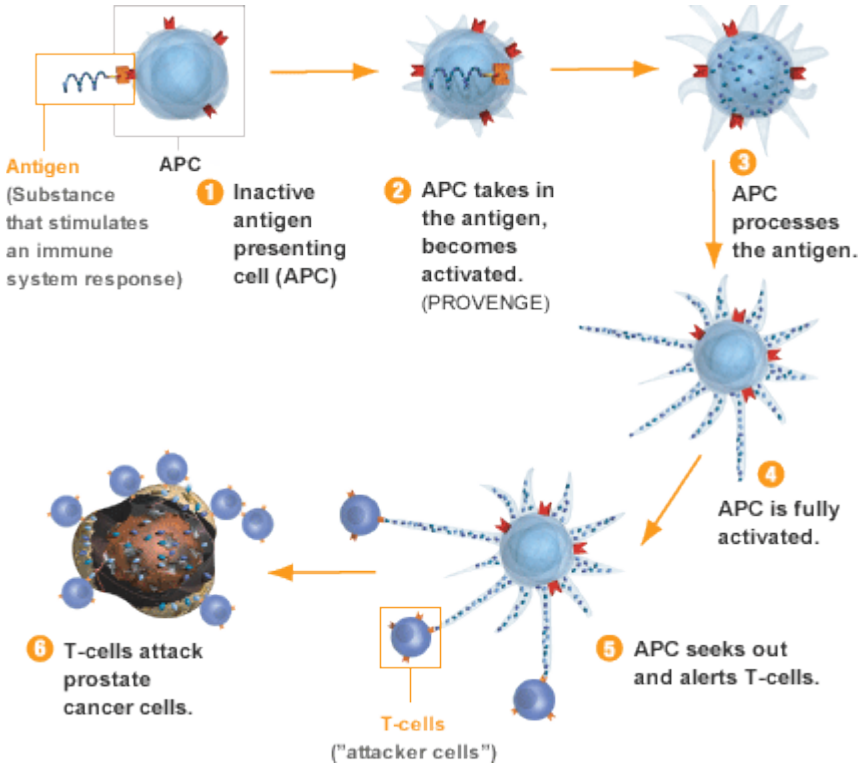

Figure 1.2. The approach for APC-based vaccination relies on eliciting robust maturation ex vivo and the relaying of an immune response to T cells. Important factors, not diagrammed, include identification of an ideal subset of APCs, including class and maturation, and identifying an effective mechanism of delivery of mature APCs to T cells. These two considerations are two of numerous motivating factors for migrating to a T cell-based approach.

the number of transfusions and latent time between transfusions [6-8]. In the interest of increasing the fraction of cells that successfully migrate to lymph nodes to active

downstream cells, other studies have looked to artificially mature DCs *in vivo* [9, 10]. The sheer number of considerations and any associated interdependencies has complicated previous attempts to use DCs as a medium for immunotherapy. The diversity in clinical design that all aim to optimize these considerations has complicated a meta-analysis of the endpoints that could help in identifying key parameters. Ultimately, the complexity of APC manipulation has led to conceptually sound yet practically ineffective therapies. This disparity was dogmatized as a failure to translate scientific merit into clinical endpoints; though DC transfusions showed persistence of transfused cells, tumor metastases were not greatly diminished, and the best cases demonstrated a lack of further metastasis and primary tumor growth: neither endpoint being positively reflected by Response Evaluation Criteria in Solid Tumor [RECIST] guidelines. These attempts culminated with a single clinical success, Provenge, though it has had questionable commercial success as regulatory boards and insurance companies continue to question whether its marginal efficacy over current therapies justify the exorbitant cost of a personalized therapy.

Currently, DCs remain an attractive medium to modulate an immune response. However, new technologies such as monoclonal antibodies and chimeric antigen receptors [CARs] are supplanting the role of the APC, enabling the activation of T cells in a process that is free of APCs. Migrating to a T cell-based therapy mitigates many of the concerns regarding APCs previously mentioned: in particular, the requisite for substantial migration to lymphatic tissues, where naïve T cells await activation. However, a T-cell based therapy also necessitates a more controlled approach, as the APC must be emulated

in vitro. This aspiration requires a depth of understanding on the activation process through which T cells are matured and an appreciation for the functional role of the T cell being used.

1.3. The CD4+ helper T cell

In the context of immunotherapy, T cells provide a compelling cell therapy. The role of CD4+ T cells, also referred to as helper T cells, can best be described in juxtaposition to CD8+ cytotoxic T cells [CTL]. Whereas CTLs are characterized by their capacity to directly engage pathogens, helper T cells take an indirect approach to immunity. CD4+ T cells instead focusing on tasks such as cytokine secretion and immune cell interactions to direct and hone the response of other immune cells.

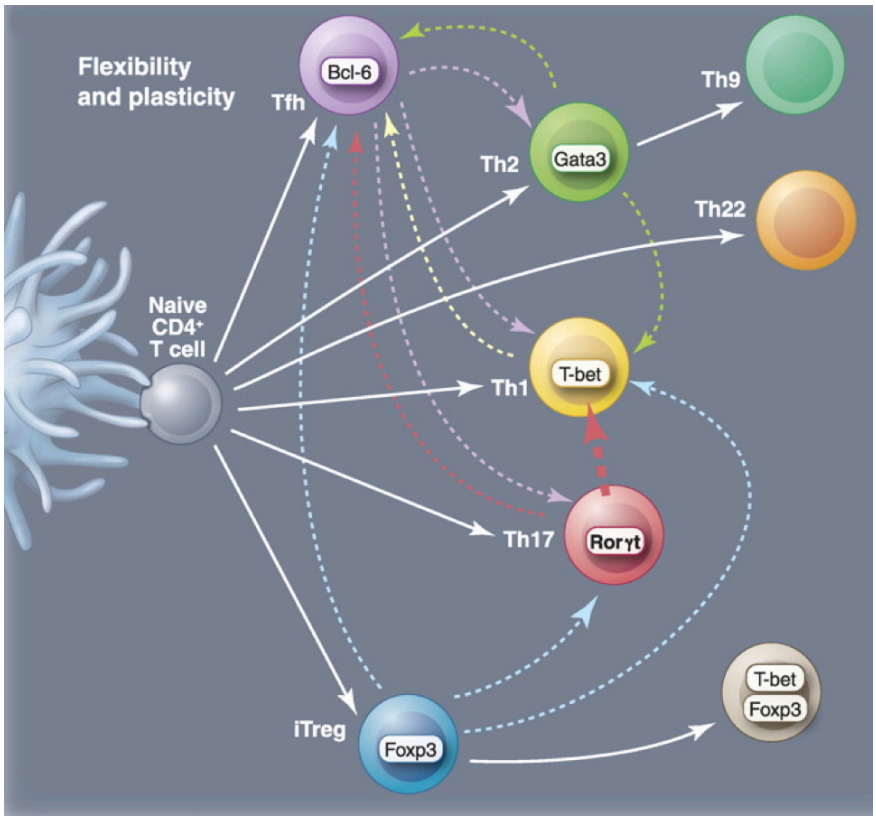

Figure 1.3. A schematic indicating the numerous pathways available to a naïve CD4+ T cell following activation (white arrows). Each of these subsets is hallmarked by one or two key cytokines, though numerous situations may arise where T cells change their cytokine profile (blue, red, violet, yellow and green arrows). T_H subsets T_{fh}, T_{H22}, T_{H9} and T-bet+ T_{reg} cells are not mentioned in this discussion, though their unique roles further highlight T cell plasticity.

To facilitate its role in crafting an adaptive immune response, naïve T cell plasticity enables numerous viable pathways. Initially, two CD4+ subsets, T_h1 and T_h2, were characterized as mature derived states resulting from cellular activation; these two phenotypes were found to respectively enhance cellular immunity and humoral immunity [11, 12]. Both responses are potent and are in line with the role of CD4+ T cells as facilitating in a coordinated response with other immune cells. Later, two additional subsets, T_h17 and T_{reg}, were also found to derive from activation, though these two CD4+ subsets are tautologically named for respectively augmenting inflammation via IL-17 secretion and immunoregulation [13, 14]. Mounting evidence has more recently demonstrated that T cell plasticity occurs in these mature subsets, and that commitment to one of these pathways was not irreversible; rather, crossover between different roles and surface expression of receptors indicative of numerous subsets was not uncommon (Figure 1.3) [15]. This plasticity is not always advantageous; many T_h1 and T_h2 T cells lose function when in the presence of T_{reg} cells and through mechanisms used to suppress an immune response, T_{reg}s can tolerize these cells to a neighboring tumor [16, 17]. An understanding of the dynamics involved in CD4+ T cell post-activation plasticity would be advantageous in either preventing or directing the direction of T cell fate and function. Moreover, what effects cellular activation may have on cell plasticity are still under

investigation. A deeper understanding of T cell activation would facilitate these studies.

1.4. Immune Synapse kinetics

T cell activity is initiated by successful contact and education by an APC. The interface between these two cells, the immune synapse [IS], is the site where extensive information is relayed between a T cell and its activating APC (Figure 1.4 A). Its highly regulated and structurally complex method for directing T cells towards one of its multifarious fates is mediated by the synchronization of interrelated proteins. The epicenter of the interaction is the presentation of an antigen by the major histocompatibility complex [MHC] on the APC to the aptly named T cell receptor [TCR] on the T cell. Receptor engagement is followed by central clustering of MHC and TCR molecules in the APC and T cell respectively. Other surface molecules either centrally migrate along with these two or are segregated to the periphery of the interaction, leading to the formation of spatially discrete zones of supramolecular activation clusters [SMACs] that resemble a bull's eye pattern (Figure 1.4 B). In a mature synapse, receptor zone correlates with ectodomain size, where the receptors with the larger ectodomains are pushed to the peripheral SMAC [pSMAC] and those with smaller ectodomains localize to the central SMAC [cSMAC]. Movement occurs in discrete bundles, or microclusters, that are often comprised of multiple receptors. On the T cell surface, TCR-MHC complexes migrate to the central region of the bull's eye, or central supramolecular activation cluster [cSMAC]. Costimulatory factors further augment a TCR-derived activation, polarizing the response

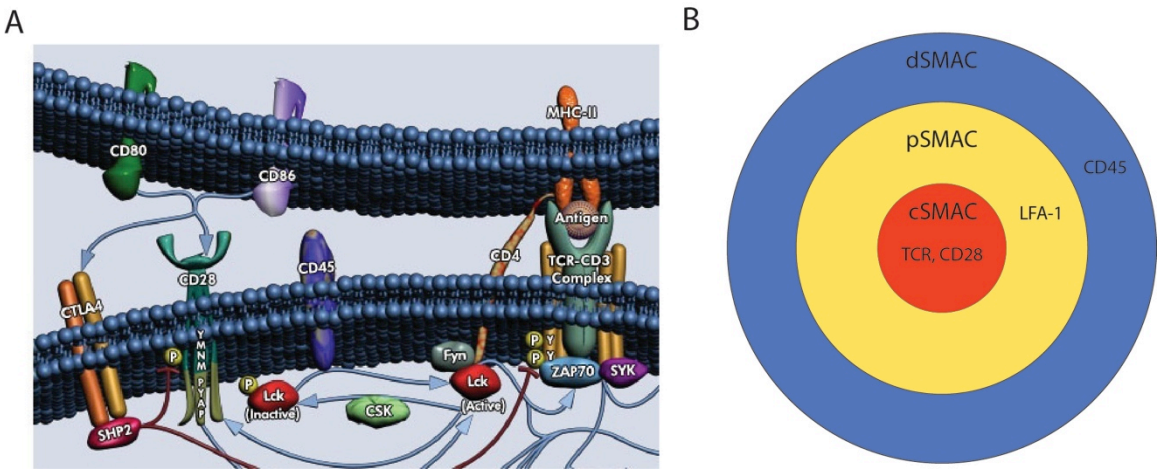

Figure 1.4. (A) A diagram indicating some of the key players involved in CD4+ T cell activation by an APC. Interactions of note include the TCR-CD3 complex interacting with the MHC class II and the interaction of CD28 with either CD80 or 86. In this diagram, intracellular T cell complexing of these two receptor pairs is mediated by Lck, though other Src kinases, including Fyn, are also capable of mediating this interaction. (B) A schematic of the T cell IS. The central SMAC contains activating factors (ie TCR, CD28), the peripheral SMAC contains adhesion factors (ie LFA-1) and distal SMAC is the region where CD45 is excluded to limit its role during T cell activation.

of the accepting T cell to either target the presented antigen, as is the case with positive costimulation by CD28, or to tolerate the antigen, which occurs with CTLA-4 mediated antagonism. These two receptor pairs both rely on activity of downstream constituents, including Src kinases and Phosphatidylinositol3-kinases [PI3K], to propagate their influence on T cell fate. How costimulation is mediated through intermediaries is critical in the harnessing of an immune response to target disease.

In addition to the competing dynamics that occur within the T cell, there are a number of APCs that are capable of directing T cell activation, including B cells, macrophages and DCs. The junction of a T cell with each of these APCs results in a distinct IS which

differentially directs the programming and ultimate function of the T cell. Of these potential APCs, DCs are the most robust and perhaps the best understood, though work exploring their interfacing with T cells has only begun in the past few years [18, 19]. A change in the APC or the antigen it presents is known to direct T cell fate; what is responsible for this change and the role of the IS in this process is still being studied. In addition to the intracellular biomechanics that drive T cell activation, it has been postulated that the mechanical properties of these different APCs may drive cellular activation. In this context, we explore the mechanical response of T cells to activation, a process that while beginning with transmembrane domains located at the cell surface, is largely dependent on the underlying cytoskeletal structure. A study into the mechanics of the cytoskeleton during activation will facilitate a mapping of an IS-driven T cell mechanoresponse.

1.5. Cellular Activation and the Role of Spatial Interplay

Receptors segregate into the mature IS based on ectodomain size, facilitating sustained interactions of receptor pairs that would otherwise be sterically impaired. Though the function of the IS relies on differences in ectodomain size, its formation and sustainment is driven by intracellular dynamics. However, the formation of a mature synapse is not a requisite to trigger downstream signaling, particularly as the time course for IS formation does not appear to coordinate with other events critical for T cell activation, including TCR crosslinking, Ca^{+2} flux, and tyrosine phosphorylation [20]. Microclusters of TCR, submicron vesicles containing roughly 30-300 TCR molecules form prior to their migration to and eventual formation of the cSMAC, implicating their role in the initiation

of downstream signaling [21, 22]. Moreover, the comigration of CD28 with TCR in microclusters suggests that the fundamental components necessary to polarize a cellular response to positive costimulation are already in spatial proximity prior to mature IS formation [23]. The reorganization of these microclusters to the hierarchical mature IS is a process that is understood to be driven by the cytoskeletal network; however, the mechanism for this process is still a subject of study.

Numerous research groups, including our own, have employed soft lithography to control the spatial localization of activating signals in artificial synapses as a method of resolving the role of spatial proximity (Figure 1.5 A) [24-26]. This work has demonstrated that the relative positions of TCR and CD28 within the synapse impacts high-level function, measured by the translocation of NF-κB and the secretion of the cytokine IL-2 [24]. In an effort to further resolve the complexity at work, as well as to develop more relevant preclinical models, preliminary studies in our research group have revealed differential sensitivity to the spatial arrangement of costimulatory factors in primary

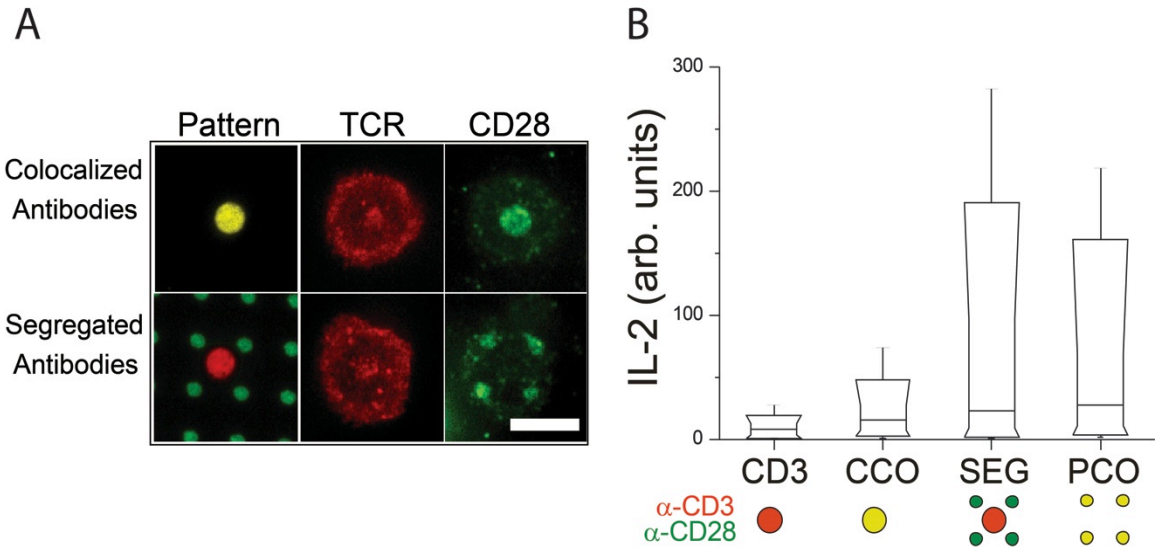

Figure 1.5. Segregation of costimulatory signals. (A) Soft lithography is employed to localization activating antibodies in desired patterns (left column) and result in the distinct localization of the complementary protein (middle and right columns). (B) IL-2 secretion by mouse CD4+ T cells is measured on patterned surfaces at six hours, and demonstrate that colocalization of antibodies targeting CD3 and CD28 [CCO] enhance activation relative to TCR triggering alone [CD3]. Presentation of these antibodies over a wider area further enhance IL-2 secretion, whether these antibodies are segregated by micron scale distances [SEG] or colocalized peripherally [PCO].

T cells from mouse and human sources. In particular, whereas mouse T cells demonstrate an ability to integrate costimulatory signals across artificially engineered micron scale regions, human T cells fail to integrate costimulatory signals across comparable distances. This disparity presents an opportunity to better characterize the role of spatial organization in cellular activation, as well as to identify the underlying mechanisms in which spatial sensitivity is differentially conferred in the two species. The following chapter will further address the role of TCR and CD28 spatial crosstalk in T cell costimulation.

1.6 Cellular Adhesion and Force Generation during Cellular Activation

One of the approaches that has been used to resolve the process of IS formation is the simulation of the APC with a planar lipid bilayer that is supported on a glass surface and contains the fundamental components for initiating T cell activation. In a set of experiments where actin velocity was tracked during synapse formation, Yu et al. demonstrate that centripetal actin flow reduces in speed when passing confined TCR cluster regions [27]. The lack of a complete halt in speed does suggest that there are no strong interactions between the TCR and actin, and the reduction in speed is consistent with a model that has transient interactions. The source of this actin has previously been identified to be retrograde flow from lamellipodia that eventually depolymerizes upon reaching the center of the synapse [28, 29]. This change in actin retrograde velocity is one metric for identifying the role of the cytoskeleton though ultimately proves difficult to establish for direct quantification. In addition to transient changes in actin flow, numerous microclusters, some distinct from TCR clustering, have also been found to associate with this actin retrograde flow [19, 21, 30]. It is compelling to consider that the degree of centripetal motion of these clusters may be correlated with their relative extent of association to the actin cytoskeleton: those that migrate further inwards having a greater association whereas those that experience little migration have a weaker association. Future work along this direction may yield insights into the nature and mechanism of cytoskeletal associations with IS microclusters.

Research endeavors from other groups have looked to quantify the total force exerted by

cell upon TCR triggering [31]. Husson and colleagues examine the coordination of cellular force generation and other early components of cell activation, including calcium flux and actin relocalization. Though demonstrating that TCR triggering does indeed lead to force generation, the method of analysis resulted in a single, bulk metric for a pushing or pulling force. Moreover, the contact area was restricted to 2.8 μm, the size of antibody-coated bead used to probe cellular forces. More recently, Ueda and colleagues have shown that T cells extend numerous invasive filopedial structures that penetrate deeply into activating APCs [32]. Though their work utilized fixed cells measured through electron microscopy, these protrusions suggest that force generation is dynamic. Evaluating cellular force exertion as a single metric makes for an adequate initial estimation of T cell mechanics; however, more fine-tuned techniques are needed to probe the underlying mechanisms at play during cellular activation.

The work presented in this thesis will more directly quantify the forces that the cytoskeleton generates during cellular activation, looking to assess the total force exerted by a T cell while also retaining resolution of local forces. By exploring both the global and local forces triggered by APC-based activation, there is great opportunity to ascertain behavioral trends during the activation process. Resolving these aspects will lay the groundwork for identifying what cellular constituents are involved in the multifaceted process of T cell activation. Specifically, this system will be applied in a study of CD28 and its contribution to force mechanics upon integration with TCR signaling.

1.7. Cancer Dissemination

A robust immune response requires policing of all regions of potential host infection. Thus, a large number of leukocytes must routinely transverse into peripheral tissues to identify or target pathogens. Other than a small number of exceptions, leukocytes can penetrate vascular and peripheral tissues with relative ease. This phenomenon has come to light when studying the metastatic properties of cancer cells, whose migratory patterns do not follow the canonical migratory pattern documented for fibroblast cells. It has instead been proposed that certain cancer cells emulate leukocytes when migrating across epithelial membranes. Even our most well-articulated categorization for a phenotype cancer exhibits a strikingly wide degree of genotypic heterogeneity. Thus, a deeper understanding of the migratory models for both fibroblasts and leukocytes, including a comparison of similarities and differences, is critical. To this effect, we propose to develop a reproducible and robust system to study the transmigration of leukocytes. Initial work will focus on behavioral characterization as well key proteins that are relevant to the process.

1.8. Impact and Significance

A number of factors motivate the development of tools to further control T cell activation. Perhaps of paramount importance is the potential to treat diseases that have eluded traditional small molecule pharmacology. By harnessing the high specificity of immune cells, there is great ambition to cultivate immune cells in situ for use in personalized treatments that escape the limitations of small molecule-based strategies. Past pharmacological approaches could claim some small success towards improving the outlook for patients diagnosed with cancer. Likewise, cancer diagnosis often occurs too

late for substantial benefit from surgery; even in situations where the cancer is diagnosed during its onset, remission is an ever-persistent concern with surgical excision of metastases. Substantial improvements in cancer patient quality-adjusted life years [QALY] were first realized with the advent of monoclonal antibody therapies: one of the earliest instances of harnessing the immune system in a non-vaccination therapy. A deeper understanding of T cell activation and further work in the direction of immunotherapy will blur this difference between biotechnology and vaccine therapies in the encompassing field of cell-based therapies. A similar rationalization may be applied to the time and effort dedicated towards HIV. Though pharmacological drugs may deter the progression of the disease to the extent that CD4+ cell count is undiminished, they have been unsuccessful in enabling the immune system to recognize and eliminate the viral load. Moreover, these treatments require daily regimens, compounding both costs and adverse side effects. For both cancer and HIV, a number of promising successes have indicated that these aspirations are not baseless [33-38].

The work entailed in this thesis seeks to buttress these successes by providing insight into what has made them successful. The subsequent chapters will focus on the CD28 costimulation pathway that is critical for functional T cell differentiation. This work looks to resolve the process through which CD28 initially couples with TCR-based activation and deconstruct the pathway through which CD28 mechanically augments cellular activation. Moreover, this thesis will identify and characterize underlying differences in mouse and human primary CD4+ T cells that may be applied to more effectively bridge preclinical work with clinical trials.

Chapter 2 - Lck Mobility Confers Spatial Sensitivity to Cellular Activation

2.1 Abstract

APC-driven T cell costimulation involves the formation of a spatially complex synapse. Previous work has identified that the relative position of CD28 within the immune synapse drastically augments the secretion of IL-2 by mouse CD4+ T cells. In contrast, human cells fail to integrate TCR and CD28 signaling when segregated on the micron scale. Moreover, previous work demonstrates that mouse cells are sensitized to spatial segregation of these receptors through the immobilization of Cholera Toxin subunit B [CT-B] at the interface. The proposed mechanism for this extracellular manipulation of intracellular mechanics is the immobilization of cholesterol-rich regions, with which certain intracellular proteins associate. The observed disparities in high level function, IL-2 production, were also found to correlate with the distribution of the Src kinase Lck in its active form, which shows substantial distribution across the interface of mouse cells but remains highly colocalized with TCR activation in human cells. This chapter characterizes the role of Lck diffusion in differentially integrating TCR and CD28 signaling, as well as the ability of CT-B to deter Lck diffusion in mouse cells. Cytoskeletal enrichment to the activating interface in the two systems reveals substantial differences. Human cells exhibit a more dense cytoskeleton at the IS than mouse cells and CT-B slightly augments the cytoskeleton of mouse cells. Disassembly of this cytoskeleton in human cells through chemical inhibition both modifies the diffusivity of Lck and desensitizes them to segregation of TCR and CD28 signaling. Together, these results demonstrate a reaction-diffusion model for regulating intracellular signaling

where both membrane dynamics and cytoskeletal restructuring play significant roles in relaying T cell activation.

2.2 Introduction

The immune synapse forms through the coordinated effort of both the T cell and its APC. Antigen presentation by the APC to the TCR designates it as the major coordinator of cellular activation and the centerpiece of the IS. However, TCR engagement is alone insufficient for cellular activation. For full elicitation of T cell activity, a costimulatory factor is required. CD28 was the first discovered costimulatory factor, and its engagement by APC receptors CD80 or CD86 complements TCR activation to produce a robust and profound response in the naïve T cell [39-41]. The synergism of the TCR and CD28 pathways depends on numerous downstream components, the coordination of which can drastically skew the direction of cellular activation.

Lck is known to play a significant role in the activation of both TCR and CD28 receptors. Upon TCR engagement, Lck is the first kinase to initiate tyrosine phosphorylation of the ITAM motif of CD3ε, enabling recruitment of Zap-70 and basal cell activation through the TCR. In addition to mediating activity of the TCR-CD3 complex, Lck also plays a role in enabling downstream signaling of CD28 through tyrosine phosphorylation of its cytoplasmic tail [42, 43]. The 41 amino acid cytosolic tail of CD28 mediates numerous functions, including but not limited to: altering cellular metabolism, activating transcription factors, inducing cytoskeletal rearrangement, polarizing cells towards T_H2, circumventing anergy and cytokine secretion [44-46]. These processes, collectively,

signify CD28-based costimulation as a significant factor in the maturation of T cells and motivate research that delves into the processes involved to enable CD28-based costimulation.

Previous work has demonstrated that mouse CD4+ T cells could respond to micrometer-scale segregation of the CD3 and CD28 receptors, suggesting that Lck was capable of relaying costimulation even over long-range distances within the cell [24]. Human CD4+ T cells have also been revealed to be incapable of eliciting costimulation when receptors are separated in the same manner, affording an opportunity to assess the underlying mechanism of Lck-mediated costimulation through a study of the two systems. This concept of modulating cellular activation through manipulation of IS structure implicates that regulation of intermediate signaling molecules as key in conferring spatial sensitivity. Both regulation of lateral diffusion and protein phosphorylation states have been described as viable mechanisms in other systems [47-49]. Moreover, the significance of spatial interplay in the IS is not without prior merit. Previous work looking at T cell activation by B cells and DCs shows differential localization of the TCR with CD80, one of two binding partners on APCs that engage the T cell costimulatory receptor: indicating that different APCs differentially regulate the microscale segregation of the TCR with CD28 [18, 50]. In this aim, we focus on the CD4+ T cell and the mechanisms through which spatial sensitivity are conferred.

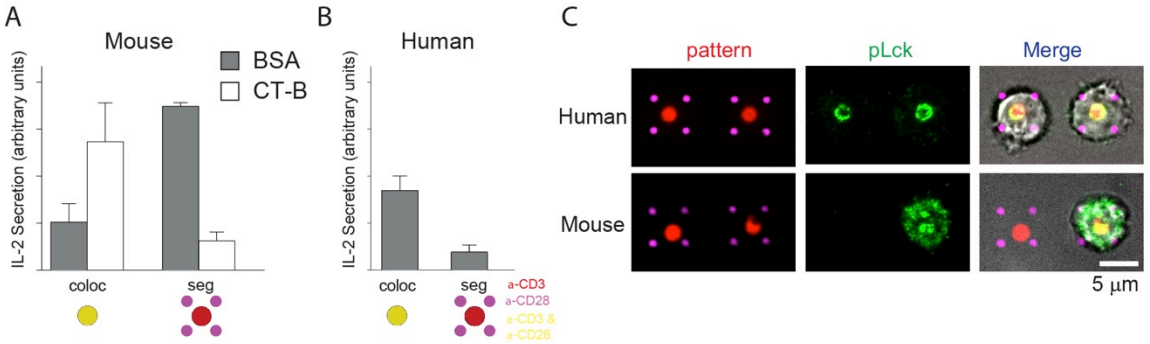

Figure 2.1. Spatial Sensitivity to Costimulation. (A) IL-2 is measured at six hours in mouse CD4+ T cells on surfaces that target CD3ε and CD28 in colocalized (coloc) and segregated (seg) patterns. With a background composed of ICAM-1 and BSA (BSA), localization of CD28 to the periphery of the interface enhances secretion. However, when cholera toxin subunit B (CT-B) is used, secretion of IL-2 is severely curtailed on segregated surfaces. (B) Unlike mouse cells, human T cells show reduced IL-2 secretion at six hours upon segregation of CD3ε and CD28 signaling. The level of IL-2 secretion is comparable to surfaces that do not contain CD28. (C) Staining for active Lck, distinguished by phosphorylation at Tyrosine 394 (pLck), shows differences in mouse and human cells on segregated surfaces. Whereas mouse cells (bottom) show a relatively homogenous distribution, human cells exhibit preferential localization of pLck with sites of TCR activation. Scale bar denotes 5 µm.

Colocalization of CD3 and CD28 through microcontact printing result in relative high levels of Interleukin-2 [IL-2] secretion in murine T cells, though the spatial segregation of these two pathways resulted in substantially higher levels of secretion (Figure 2.1 A). Introduction of surface-immobilized CT-B reversed this trend: enhancing activation on colocalized features and substantially reducing the benefits initially conferred by separation of the two receptors (Figure 2.1 A). Though the precise mechanism is still under investigation, the application of CT-B as a stain for monosialoganglioside [GM1]-rich regions suggests that cholesterol-rich regions of the membrane may be involved in

protein shuttling. Moreover, Lck preferentially associates with GM1, a process which is thought to dissociate Lck from its strong interaction with CD4 so that it instead migrates with GM1-rich membrane microdomain [51].

Like mouse cells, human CD4+ T cells demonstrated high levels of IL-2 secretion on colocalized patterns. However, the spatial separation of the two receptors in human cells substantially reduced IL-2 secretion in the absence of CT-B treatment (Figure 2.1 B). Immunostaining for phosphorylated Lck provides strong correlative evidence that while active Lck localizes with both segregated TCR and CD28 in mouse cells, it is predominantly constrained to the site of TCR activation in human cells (Figure 2.1 C). Additional work will assess the mobility of Lck during cellular activation and seek to understand the underlying factors that contribute to this inter-species difference.

2.3 Materials and Methods

Surface Preparation. The preparation of micropatterned glass surfaces has been previously demonstrated and validated, both by this lab as well as others [24, 52, 53]. We recommend these cited literatures for details on fabricating these surfaces. Briefly, this process involves fabrication of the desired features through photolithography, and the application of soft lithography to transfer protein(s) of interest in structural patterns that conform to these features. Given the relative stability of antibodies, multiple rounds of transfer are possible within a defined space. This work applies at most two rounds, with the interest of segregating activation of the TCR and CD28 receptors to their respective antibodies using microcontact printing. Following patterning of antibodies targeting

CD3ε and CD28, the background of a patterned surface is backfilled with F_c-ICAM-1 (R&D Systems, 720-IC-200) at a coating concentration of 2 μg/mL. For experiments where CT-B (Invitrogen, C-34779) was used to deter membrane mobility, either CT-B or BSA was mixed at a 1:5 ratio with ICAM-1 for an effective concentration of 0.4 μg/mL. To ensure consistent coating and imaging techniques, glass coverslips were cleaned in 200°C detergent (Linbro 7x, diluted with DI water to working concentration), rinsed in multiple rounds with MilliQ-purified water and subsequently baked at 415°C overnight.

Cell Isolation and Culturing. Resting peripheral human CD4+ T cells were isolated from whole blood. Following venipuncture, primary lymphocytes were isolated from whole blood by Ficoll-Paque gradient (GM) using an Eppendorf 5810R swinging bucket centrifuge. CD4+ T cells were enriched from the lymphocyte layer by negative selection using Invitrogen Dynalbeads Untouched kit (Invitrogen 113-52D). Mouse CD4+ T cells were isolated separately from lymph nodes and spleens of C57BL/6 mice aged 6-8 weeks. After an initial extraction through a 40 μm filter, CD4+ cells were enriched similarly to human CD4+ T cells, via negative selection using Invitrogen Dynalbeads Untouched kit (114-15D).

CD4+ T cells were cultured in RPMI 1640 media supplemented with 10% FBS, 10 mM HEPES, 50 U/mL Penicillin & Streptomycin, 2 mM L-glutamine and 50 μM β-Mercaptoethanol. For timelapse microscopy, phenol red was excluded from the media to minimize autofluorescent interference. For experiments, cells were cultured for 30 minutes to eight hours at 37°C, 5% CO_2; temperature and gas concentrations were

maintained using a LiveCell™ stage top incubation platform. Phenol-free RPMI 1640 media was used during microscopy to minimize autofluorescence.

For experiments involving F-actin destabilization through Latrunculin B [LatB], cells were given 15 minutes to bind to the surface prior to LatB treatment. A range of LatB concentrations, from 10 nm to 10 μm, were tested to discern a concentration that was effective at moderately destabilizing the cytoskeletal, permitting a notable effect without detracting from basal processes. These starting values were determined from the manufacturer product sheet as well as previously published literature using LatB in lymphocytes [54-56].

Antibodies, Proteins and Immunostaining

Both human and mouse T cells were activated using monoclonal antibodies targeting the CD3ε chain of TCR and CD28. OKT3 and CD28.6 were used for human cells; CD3ε clone 145-2C11 and CD28 clone 37.51 were used to activate mouse cells. An F_c-ICAM1 chimera was used for LFA-1 interactions. An F_c variant is ideal for our experimental setup, as its adsorption to planar surfaces can compete equitably with the TCR and CD28 activating antibodies used.

For measurement of CD4 diffusion, F_{AB} regions were generated by using Pierce F_{AB} microprepartation kit (Pierce, 44685). The use of the F_{AB} regions permit a more transient binding duration than a traditional dimeric antibody, helping to mitigate artifacts induced through the labeling process. F_{AB} regions were added to the cells following seeding at a

concentration of 100 nM.

For immunostaining, cells were fixed with 4% paraformaldehyde for 10 minutes and the membrane then permeabilized with 0.1% Triton X-100 in phosphate-buffered saline [PBS] for 15 minutes. Antibodies targeting phosphorylated Lck Y394 (Novus Biologics, NBP1-60894), or total Lck (Cell Signaling, 2714) were used. Cells were also stained for with phalloidin (Invitrogen, A12379) to resolve F-actin.

IL-2 Assay. Cellular activation is quantified in the context of the secretion of the cytokine IL-2: one of the key indicators of CD4+ T cell activation and a functional mediator of its effect on other cells once active [57, 58]. One of the advantages of using IL-2 as a proxy for cellular activation is early onset of IL-2 production following cellular activation. IL-2 is measured by indirect capture through a Miltenyi Biotec secretion assay which, through an indirect capture via the ubiquitous transmembrane protein CD45, allows measuring of IL-2 secretion on a cell-by-cell basis. This discretization permits a measurement of IL-2 on patterned surfaces in a manner that would be less robust via ELISA measurement. As per the protocol recommended by the manufacturer, cellular activation on microscale patterns began at six hours, which is adequate time for the cell to initiate substantial IL-2 secretion, and lasted for one hour. Thus, the rate of IL-2 secretion was measured for one hour, lasting from the 6^{th} to 7^{th} hour of cell adhesion. For experiments where IL-2 secretion was measured in LatB-treated cells, the 15 minute wash-in time was encompassed in the overall six hours. LatB was also applied during the subsequent hour of IL-2 measurement, as this study does not aim to quantify the recovery

process of LatB-treated cells.

Nucleic Acid Transfection. The vectors used in this section include a construct for Lck appended to the fluorescent protein YFP, both in plasmid and mRNA form. DNA plasmid and mRNA based methods were both used and found to be robust. Transfection was performed using Neon Transfection System by Invitrogen. Following transfection, cells were permitted to recover in prewarmed RPMI 1640 media containing 10% FBS and 5mM L-glutamine. For plasmid-based transfection, cells were left to recover overnight, whereas for mRNA-based transfection, cells were left to recover for 5 hours before imaging. Experiments involving FRAP of transfected cells were given 15 minutes for initial adhesion and FRAP data was collected in the subsequent hour, except for instances where otherwise stated in the experimental design.

Diffusion Measurement. Diffusion was measured via fluorescence recovery after photobleaching [FRAP] to gauge the recovery of a subcellular region across the glass-cell interface. Images were collected by Total Internal Reflection Microscopy [TIRFM]. TIRFM relies on a change in refractive index between a glass substrate and media to excite fluorophores that are within the vicinity of the interface: permitting a depth of view within 50-100 nm of this interface. Lck is a cytosolic protein that associates to membrane components; thus, TIRFM enables imaging of the membrane fraction of Lck while excluding the larger cytosolic fraction.

Data Acquisition and Analysis

All images were collected using an Olympus IX81 inverted microscope equipped with objectives for imaging at 20x, 60x and 100x resolution. Images were collected using an Andor iXon3 EM-CCD for time-lapse microscopy and an Andor Neo cSMOS for high resolution microscopy. MetaMorph for Olympus was used for software acquisition of images. Image processing was predominantly performed with ImageJ v1.46, included but not limited to: overlaying multiple channels, measuring cell area and intensity, bleach-correcting timelapses and generating montages. Where appropriate, certain functions of image analysis were performed in Matlab.

Diffusion coefficients were measured using the Hankel transform, as described by Hook and colleagues [59]. This process makes use of the Hankel transform to calculate a weighted-sum of linear diffusion profiles radially distributed around the central point of bleaching. There are numerous benefits for calculating recovery by diffusion with the described method. In brief, these benefits include: independence from an analytic solution, reduced sensitivity to boundary conditions (relative to Fourier method), and the ability to resolve anisotropic diffusion. In the absence of anisotropic diffusion, a weighted average of the diffusion profile may instead be used.

Statistical Analysis. Statistical analysis was performed using a number of techniques. A p-value of 0.05 was used unless stated otherwise. A t-test was executed on paired analyses. The validity of multiple comparisons was corrected for with Tukey's range test. Data was recorded in Microsoft Excel 2011 and statistical analyses were performed in

Origin 8.0. Means reported in this thesis are followed with the 95% confidence value included in parentheses. All data is representative of at least two independent experimental runs, though in the interest of aligning with strict temporal parameters, multiple surfaces and discrete cell cultures are used within each independent experimental run.

2.4 Results

Lck mobility correlates with spatial sensitivity

To validate previously observed inter-species disparities, the bulk diffusion of Lck across the membrane was measured in mouse splenic and human resting peripheral CD4+ T cells. Cells were transfected with a plasmid containing Lck appended to a fluorescent tag, YFP, to measure Lck diffusion via FRAP. A visual example of this process, including the distribution of Lck prior to bleaching, the site of the bleached region and a timescale of the recovery, is demonstrated in Figure 2.2A. Employing this approach, Lck diffusion in human T cells was found to be 0.04 (+/- 0.01) $\mu m^2/s$, showing a total recovery time from a 1 μm radial bleach spot on the order of 5-10 seconds. Duplicating this process in mouse cells demonstrated a much greater capacity for diffusion, with the diffusion coefficient for Lck was measured to be 0.37 (+/- 0.09) $\mu m^2/s$ (Figure 2.2 B). This disparity in diffusivity, nearly a full order of magnitude lower in human cells than in mouse cells, fit

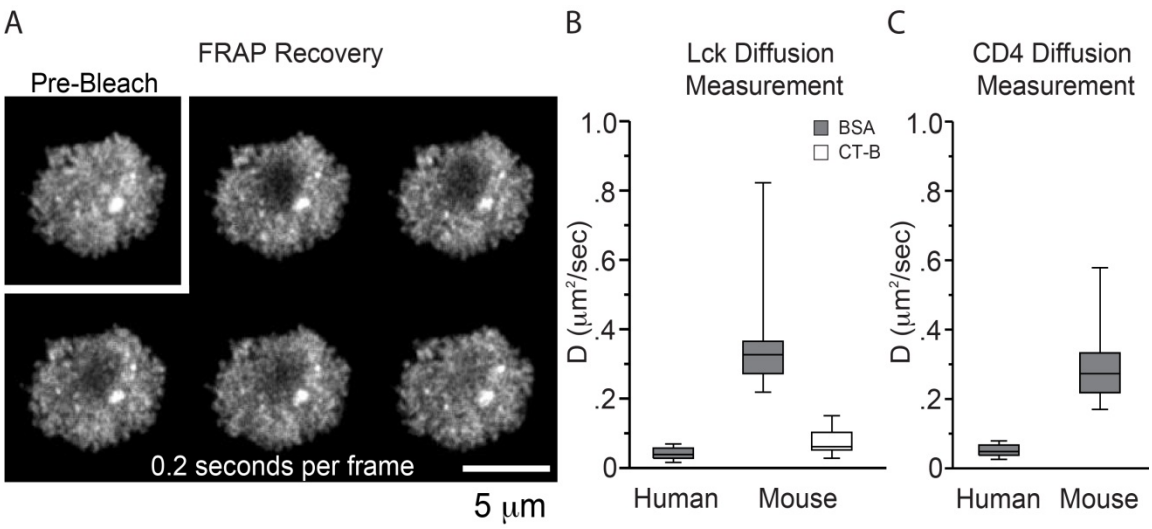

Figure 2.2. Diffusion measurement. (A) FRAP is used to measure the diffusion coefficient in a mouse T cell. The pre-bleach frame shows the distribution of Lck at the surface interface. The subsequent frame shows the result of the subcellular photobleach, approximately 1 μm in diameter. The following frames show the following timelapse. Scale bar denotes 5 μm. (B) Human T cells show reduced mobility relative to mouse cells on homogeneously coated with anti-CD3, anti-CD28 and ICAM-1. Moreover, CT-B impairs the diffusion coefficient of Lck on surfaces. To keep these ligands at a constant concentration between the two conditions, the CT-B fraction was replaced with BSA in the (-) control. (C) The diffusion of CD4 was measured and showed similar diffusive properties as Lck. CD4 diffusion in human cells was measured at $0.04 \pm 0.01\ \mu m^2/sec$ and $0.37 \pm 0.09\ \mu m^2/sec$ in mouse cells.

well with previous assumptions of a reaction-diffusion model and though it does not preclude a difference in phosphorylation dynamics, it does indicate that the diffusion of Lck is a major factor in the sensitivity of human T cells to spatial distribution of IS constituents. To further develop this model, we next looked at CT-B treated mouse cells, to see if this manipulation was successful in impairing the diffusion of Lck. Measurement of the diffusion of Lck in mouse cells when in the presence of CT-B led to a decrease in Lck diffusion, resulting in decreased mobility from 0.37 (+/- 0.09) to 0.07 (+/- 0.02)

$\mu m^2/s$ (Figure 2.2 C). This is consistent with a model where Lck diffusion is intrinsically deterred in human cells. Here, deterral of Lck diffusion through its interaction with GM1-rich lipid subdomains reflects both a diffusion coefficient as well as a spatial sensitivity to segregation of receptors that is similar to human cells. Manipulation of surface membrane dynamics through surface-immobilized CT-B augments intracellular Lck diffusion in mouse cells. This suggests either intrinsic differences in the APCs that activate human and mouse T cells or a fundamental difference in human CD4 T cells that perturbs Lck diffusion. Further exploration of these two systems focuses on the intracellular mechanisms that regulate diffusion of Lck.

Lck and CD4 exhibit a similar diffusion profile

We next looked at the transmembrane protein CD4: the namesake protein for helper T cells. The spatial correlation between Lck and CD4 is well established [51, 60]. Of note, the high affinity of Lck for CD4 and CD8 is key in the maturation of thymocytes into T cells. This affinity is anticipated to persist in naïve T cells, though a difference in the relative diffusion of Lck and CD4 in human or mouse cells would do much to rationalize the disparate behavior of Lck in the two species. CD4 also plays a role in triggering the autophosphorylation of Lck into its active state, a function not achievable by TCR coupling alone [61]. Measuring the diffusion of CD4 in the two species demonstrated a similarity in the properties of CD4 and Lck in both human and mouse cells (Figure 2.2 B, C). These results support previous works that indicate the two proteins as co-receptors, but do not contribute to an understanding of what may be responsible for the difference in cellular properties of human and mouse cells. Rather, the similarities shared by these two

proteins implicate a more fundamental difference in the two species, compelling an investigation into the underlying cellular machinery that are responsible for cellular dynamics.

Cytoskeletal Enrichment at the IS Differs in Mouse and Human T cells

Triggering of the TCR leads to extensive actin polymerization, which plays a critical role in sustained interaction between the T cell and the APC [28, 62]. To further evaluate the role of the cytoskeleton in the immune synapse, mouse and human CD4+ T cells were activated on homogeneously coated activating surfaces after which both F-actin and active Lck were stained for (Figure 2.3 A). Both quantitative and qualitative assessment

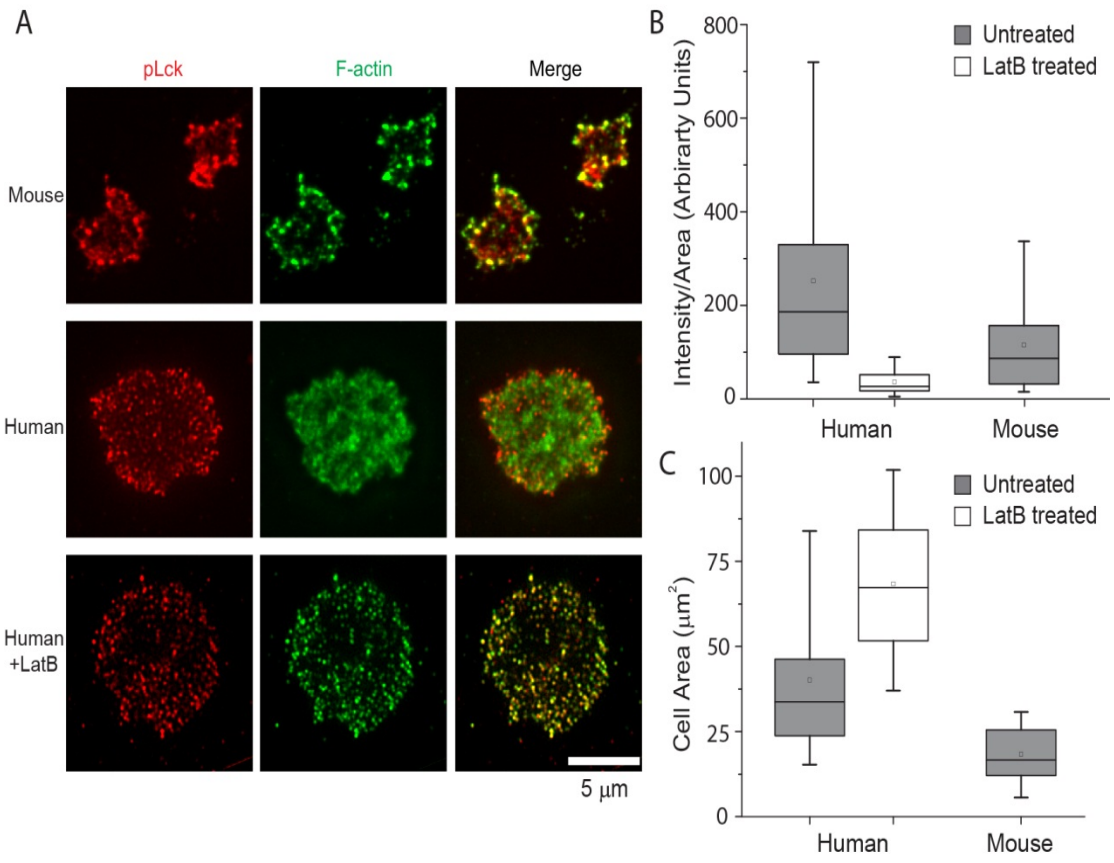

Figure 2.3. Cytoskeleton differences in mouse and human lymphocytes. (A) Mouse and human CD4 T cells were stained for phosphorylated Lck [pLck] (red) and F-actin (green) on planar surfaces coated with αCD3, αCD28 and ICAM-1, revealing distinct differences between the two species at 30 minutes. Whereas mouse cells contained enrichment of these two proteins at the periphery of the cell and a moderately diffuse network in the cell center, human cells contain a dense network of both proteins. Treatment of human cells with 1 μm Latrunculin B destabilized the actin cytoskeletal, also manipulating the localization of pLck, which now shows greater colocalization with F-actin. (B) The intensity per unit area of F-actin was greater by a factor of two in human cells than in mouse cells. Treatment of human cells with 1 μm of LatB reduced the average intensity of the actin cytoskeleton. (C) Human cells show a greater interface area, roughly twice the area, than mouse cells. LatB treatment further increases the area of human cells. Together, these quantify the degree of cytoskeletal enrichment at the IS in human cells relative to mouse cells.

revealed profound differences between the actin cytoskeletal in the two systems. Human T cells exhibited a homogenously dense cytoskeleton, rich in compact, overlapping filaments. Mouse T cell actin networks were instead characterized by enrichment along the periphery, to the extent that it severely masked low levels of actin in the central synapse. A direct comparison of the F-actin per area in the cell showed that human T cells polymerized more than twice the F-actin per area than mouse cells (Figure 2.3 B). Scaling for the size of the interface, as human T cells spread to an area twice that of mouse cells, demonstrated that the interface in human cells contained four times the amount of polymerized F-actin at the cell-surface interface than do mouse cells (Figure 2.3 C).

F-actin destabilization enhances Lck diffusion in human T cells

To test whether the actin cytoskeleton plays a role in directing Lck diffusion, we

selectively inhibited F-actin assembly with the small molecule LatB. Immunostaining of LatB treated cells confirmed phenotypic changes induced by F-actin destabilization. F-actin per area was substantially reduced, though total cell area was increased by roughly 50%, perhaps due to the inability of the cell to retain contractility with reduced levels of accessible actin filaments (Figure 2.3 A-C). This LatB-modulated diffuse network also induced a change in the localization of active Lck. Untreated human cells exhibit a dense cytoskeletal network, largely masking the spatial coordination with a far less dense active network. However, T cells treated by LatB demonstrated a high level of correlation of active Lck with the residual F-actin, their correlation tentatively suggesting an active mechanism of Lck regulation by the cytoskeleton (Figure 2.3 A). This active regulation would be in contrast to a model where a dense actin cytoskeleton passively deters Lck mobility, which would manifest with a low degree of spatial correlation between the

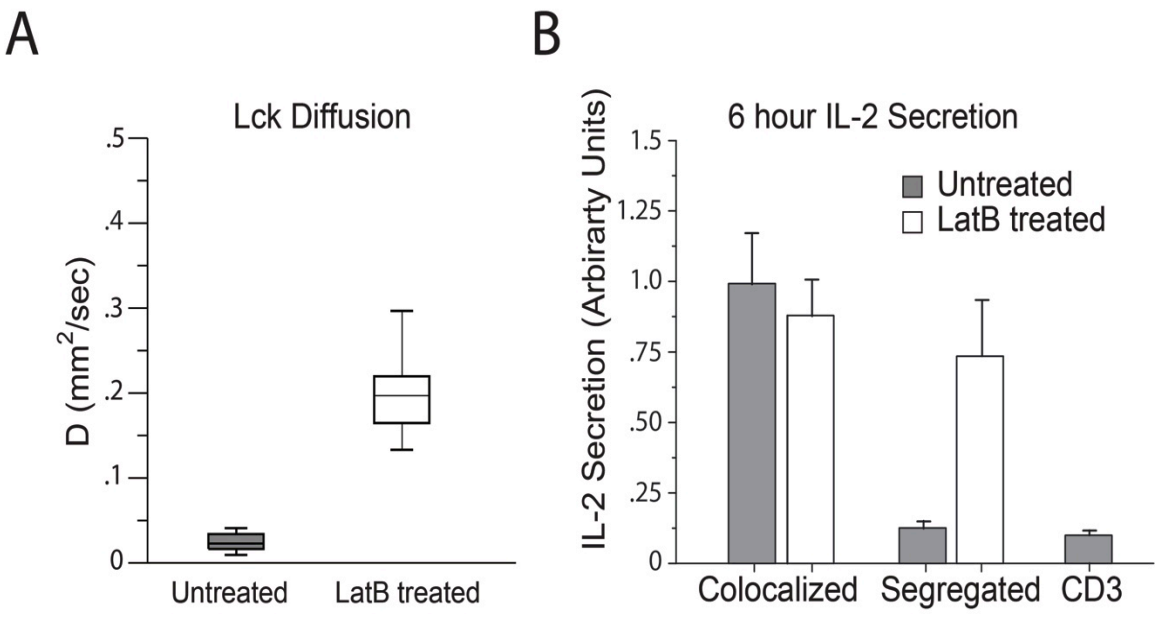

Figure 2.4. LatB desensitizes human cells to micropatterns. (A) Treatment of human T cells with LatB increases the lateral diffusion of Lck along the membrane by a factor of 5. (B) Treatment of human T cells

with LatB during the first six hours of activation does not significantly affect IL-2 production on colocalized features. In the absence of LatB, IL-2 secretion on segregated surfaces is comparable to basal activation through CD3 alone. However, LatB treatment substantially increases IL-2 production on segregated patterns, bringing secretion levels on par to those of colocalized features.

cytoskeleton and Lck. This low spatial correlation would be further reduced with the destabilization of the actin network.

To validate the role of the cytoskeleton in limiting Lck mobility, we directly measured the diffusion of Lck in LatB-treated cells. LatB-treated human cells had a measured diffusion coefficient of 0.19 (+/- 0.02) $\mu m^2/s$, compared to the 0.05 (+/- 0.01) $\mu m^2/s$ in untreated cells (Figure 2.4 A). This fivefold increase in the diffusivity of Lck indicates F-actin plays a significant role in modulating its diffusion. Briefly comparing the diffusion profile of Lck in LatB-treated human cells and mouse cells, there is still roughly a two-fold difference. The continued difference between LatB-treated human cells and untreated mouse cells suggests that the mechanism of F-actin destabilization in human cells does not perfectly reflect the mouse cytoskeletal network. Alternatively, other mechanisms of regulation are at play. This change in Lck diffusion in human cells, induced by LatB, warrants reinvestigating the capacity of human T cells to respond to patterns defined by segregation of TCR and CD28 triggering.

F-actin destabilization desensitizes human cells to segregation of TCR and CD28

To empirically test the previously observed correlation of Lck distribution and diffusion with human T cell sensitivity to segregated TCR and CD28, we measured the secretion of

IL-2 on these patterns in the presence of LatB. Using the same approach to quantify cellular activation by indirectly capturing IL-2 secretion, we measured the effects of LatB on both colocalized and segregated patterns. LatB showed little effect on colocalized features, suggesting that the concentration used to destabilize the actin cytoskeleton was sufficiently moderate to not augment IL-2 secretion (Figure 2.4 B). However, LatB treatment resulted in a profound difference on segregated patterns. Whereas untreated cells fail to couple CD3 and CD28 when these receptors are segregated, LatB treatment enabled coupling of segregated features and resulted in IL-2 production comparable to

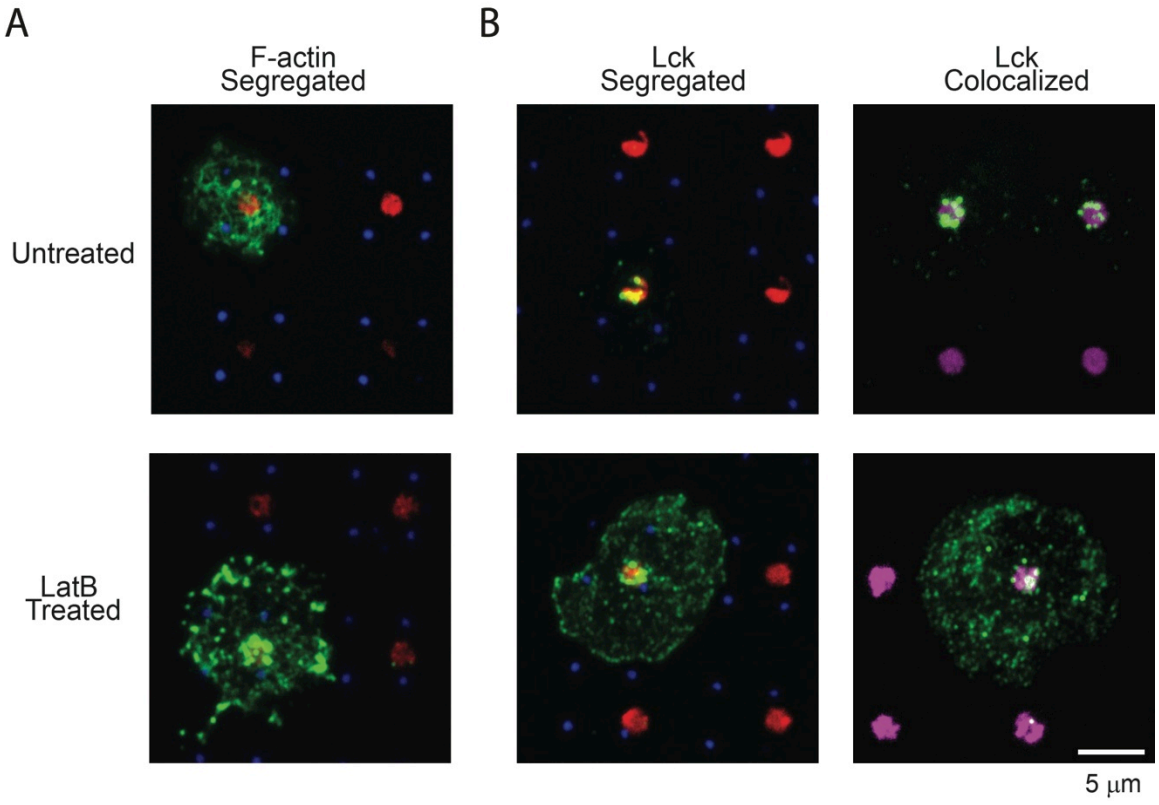

Figure 2.5. Latrunculin B modulates localization on micropatterns. (A) Staining for F-actin (green) on segregated patterns of antibodies to CD3ε (red) and CD28 (blue) shows a dense homogeneous distribution in untreated cells (top), whereas LatB treated cells (bottom) show moderate enrichment of F-actin at the site of TCR triggering and a more diffuse network throughout the interface. (B) Staining for active Lck on

segregated (left) and colocalized (right, shown in purple) features of CD3ε and CD28 both showed predominant colocalization of active Lck at the site of TCR triggering in untreated cells (top). However, treatment of cells with LatB in both instances resulted in a more even distribution of active Lck along the cell interface.

colocalized costimulation (Figure 2.4 B). These results implicate the cytoskeleton as responsible for both restricting Lck mobility and for the inability of human T cells to couple segregated activating receptor pathways. We next looked at the distribution of Lck, in its active form, on patterns to ensure that this response was indeed tied to the drastic change in IL-2 production in the presence of LatB. Staining for F-actin on segregated patterns validated that LatB leads to cytoskeletal depletion across the interface, though greater enrichment was observed near the site of TCR engagement (Figure 2.5 A). This is in keeping with previous models that point to the TCR as being responsible for the recruitment of F-actin to the interface [28, 63]. The distribution of active Lck also radically shifted in response to cytoskeletal destabilization. On both colocalized and segregated features, phosphorylated Lck showed extensive distribution throughout the cell in the presence of LatB, but remained localized to the site of TCR engagement in untreated cells (Figure 2.5 B). These results culminate this study into the role of Lck as a mediator of TCR and CD28 pathways: a process in which the cytoskeleton plays a definitive role.

2.5 Discussion

Numerous models that describe immune synapse dynamics have been developed in the

interest of understanding the process of T cell maturation; many of these models share a number of key characteristics [51, 64-67]. In the interest of vetting these models, in addition to having a sound conceptual basis for exploring the integration of costimulatory signaling within the immune synapse, we have derived a number of critical experiments to artificially manipulate cellular regulation. These results implicate that costimulation through CD28 is subjected to regulation by Lck, which confers spatial sensitivity to the TCR and CD28 receptor systems. This regulation may be described in the framework of a reaction-diffusion model, where following Lck phosphorylation at the TCR, the extent of regulation of its mobility confers sensitivity to IS spatial structure. Our observations implicate cytoskeletal dynamics and likely lipid microdomain associations as facilitators in conferring cellular recognition to microscale organization of IS receptors. Moreover, impairment of F-actin assembly in human cells via LatB inhibition does not impact T cell activation on patterns where TCR and CD28 activation is colocalized; this suggests that the abundance of F-actin at the interface is present to serve a different purpose. The following chapters will look at mechanical force generation during cellular activation: a role that the actin cytoskeleton is aptly suited to facilitate.

The work in this chapter also demonstrates that differences in mouse and human CD4+ naïve T cells responses to IS receptor segregation may be rationalized through the regulation of a mediator protein: in this context, Lck is characterized as being an ideal mediator. Human T cells restrict the migration of Lck through the development of a dense cytoskeletal network at the IS interface. This work does not directly resolve whether the mechanism of Lck regulation by the cytoskeleton is active or passive.

Immunostaining showing a correlation of the two in LatB-treated cells does suggest that there is a link between the cytoskeleton and Lck. This link, however, is not required in the context of a reaction-diffusion model: where the mode of diffusion may be either active or passive. This work does establish that destabilization of this network increases the diffusion of Lck and enables coupling of TCR and CD28 signaling across micrometer distances.

The work in this chapter also demonstrates that this model also rationalizes the lack of sensitivity for spatial segregation exhibited by mouse T cells. Direct measurement of the lateral diffusion of Lck and immunostaining for its distribution demonstrate that Lck mobility across the IS is not hindered to the extent that it is in human cells: permitting crosstalk between the TCR and CD28 pathways across micron-scaled distances. Moreover, mouse T cells feature a less complex actin cytoskeleton at the interface, rationalizing this difference in sensitivity. Previous work using CT-B to limit diffusion of Lck across the interface is also validated to result in decreased migration of Lck and to lead to slight restructuring of the actin cytoskeleton at the interface.

Given that substantial differences have previously been identified in IS formation and structure based on the APC that activates a T cell, we postulate that this insight into IS spatial complexity will prove advantageous. Our observed differences in mouse and human T cells builds on growing recognition that disparities between the two systems exist. Of particular note, T_h17 cell derivation takes different chemical cues in mouse and human CD4+ T cells [68]. T_h17 cells make for a compelling vehicle for adoptive

immunotherapy given their capacity to function even when faced by T_{reg} suppression [69, 70]. However, T_h17 cells form a small subset of the CD4+ population; devising processes to more effectively cultivate T_h17 would require careful management of activation cues in a manner that takes into consideration differences in the differentiation pathway of T_h17 cells in mouse and human models.

Chapter 3 - Characterization of T cell force generation upon activation

3.1 Abstract

The activation of T cells is a mechanoresponsive process. Numerous labs have looked to evaluate the forces that are required in the initiation and persistence of the T cell and APC interaction [31, 71]. In this chapter, we employ traction force microscopy using an elastomer micropillar array as a template that enables both the activation of T cells and the measurement of the forces they exert during activation. This system enables the calculation of cellular forces through the tracking of micropillar displacements resulting from cellular exertion. Employing this system, we first quantify the forces that T cells exert on their environment during costimulation through the TCR and CD28. Next, we assess the capacity of CD28 to act as a mechanoresponsive receptor, which is shown to augment TCR-mediated force generation. Mapping this process demonstrates that CD28 does not exhibit mechanosensitive properties, providing equivalent biophysical responses when presented in solution or on the surface material. An inhibitor-based study of the downstream components of CD28 is used to demonstrate that augmentation of TCR forces is mediated through PI3 Kinase but is upstream of the protein kinase Akt.

Unlike the previous chapter, where parallels were drawn between human and mouse systems, human T cells are the sole focus here. The substantial and rich cytoskeletal network observed in human T cells makes them ideal candidates for a study of cellular forces. More relevant, human cells were the focus of work performed with collaborators, where the proliferative capacity of human T cells was found to be enhanced by

decreasing the stiffness of the underlying substrate [72]. The work in this publication is limited to planar PDMS which, as a copolymer of two viscous materials, has practical limitations on the minimum stiffness that can be achieved. This chapter circumvents this practical limitation by using a discontinuous interface to substantially reduce this modulus, studying the behavior of T cells at a modular range that is more representative of its interaction with an APC.

3.2 Introduction

The previous chapter focuses on the signaling molecule Lck as an intermediate in harmonizing TCR activation with CD28 costimulation. The actin cytoskeleton was found to play a significant role in regulating the diffusion of Lck, conferring spatial sensitivity to segregation of TCR and CD28. Previous work has looked at the TCR interaction itself and characterized its sensitivity to force exertion: in which the actin cytoskeleton likely plays a significant role [31, 71]. Using IL-2 as an early indicator of cell activation, *Judokusomo et al.* have recently demonstrated that mouse CD4+ T cells differentially respond to the underlying rigidity of an activating surface. Though the TCR and CD28 work in unison towards cellular activation, the response to rigidity was relayed through the TCR pathway. These observations describe the summation of the first six hours of cell activation: an early time point when compared to T cell function following activation, but a time point that is downstream of the dynamics that initiate activation processes. This work characterizes the capacity of TCR to act as a mechanoresponsive receptor: playing a role in the differential transformation of a mechanical stimulus into a biochemical response.

One further step in understanding this process is to capture the process through which differential forces impart multifarious responses. A single protein that is responsible for identifying and dynamically responding to the rigidity of the underlying substrate is characterized as mechanosensitive. In the correlation of surface rigidity and six hour IL-2 secretion, it is difficult to characterize which protein is responsible for this trend. TCR and CD28 are the primary sites of engagement though for both receptors, either downstream constituents or another system acting in parallel may be responsible for this rigidity response. In this direction, we look to characterize cellular processes early on in cellular activation. Cell activation is initiated upon receptor engagement, and a large number of downstream intermediaries, such as Zap-70 phosphorylation, MTOC relocalization and Ca^{2+} flux happen within the first half hour of initial contact [73-75]. This chapter aims to use these early endpoints to assess cellular activation during the first hour of engagement. Moreover, whereas previous work has used cellular activation as an endpoint to study the effect of surface forces, this chapter aims to use cell-generated forces as an endpoint to assess cellular activation.

Force-sensing systems have previously been used as a platform to characterize cellular forces in fibroblasts and smooth muscle cells [76, 77]. Control over a large number of parameters, including substrate material, pillar diameter, pillar height and pillar spacing, enables relatively precise measurements of cellular behavior using a metric that is not easily captured by most in vitro systems: force exertion. This chapter will look at the response of CD4+ T cells to activation through the prism of mechanical forces. The

significance of this measurement has previously been articulated, where surface rigidity was shown to modulate IL-2 secretion in mouse cells. However, past work into the structure and nature of the IS has focused on metrics that have been more easy to quantify, such as the nature and organization of the proteins involved. The IS is a physical interaction between two cell types, each of which recruits a substantial cytoskeletal network to induce IS formation and retention of this interaction. Past and current techniques have enabled the identification of a majority of the key proteins involved in T cell activation; current work seeks to better characterize protein interactions and pathways. In this chapter, we first aim to directly measure cellular force generation as a function of time during TCR-driven and CD28-mediated activation. We subsequently hone in on the CD28 receptor pathway and map the mechanisms through which it physically augments TCR engagement.

3.3 Materials and Methods

Fabrication and Substrate Preparation. Masters for micropillar arrays were designed using the general template designed by the Chen lab [76, 78]. Pillars were designed to be 1 μm in diameter and were arrayed in a hexagonal formation with 2 μm center-to-center spacing to ensure equispaced proximity among neighboring pillars. Pillars of heights 3 to 9 μm were fabricated. Negative molds were cast in PDMS (Sylgard 184, Dow Corning) from these masters, silanized overnight with (tridecafluoro-1,1,2,2,-tetrahydrooctyl)-1-trichlorosilane (United Chemical Technologies) and used to cast pillar arrays directly onto thickness #0 Fisherbrand glass coverslips that were cleaned as previously described. To avoid the collapse of high aspect ratio pillars, surfaces were submerged in 99%

ethanol prior to release from their PDMS mold. The ethanol was then slowly replaced with DI water and eventually PBS containing activating antibodies that were used to coat the surface. Cast pillar arrays were assessed by SEM for vertical sidewalls and uniform pillar dimensions.

Antibodies, Proteins and Immunostaining. Human T cell activation was achieved using OKT3 and CD28.6 as previously described. For timelapse microscopy, F_{AB} regions of anti-CD45 Alexa488 (Biolegend, 304019) were used to track the cell membrane. These F_{AB} regions were generated by using Pierce F_{AB} micropreparation kit (Pierce, 44685), previously described, and added to the cells prior to seeding at a concentration of 200 nM. Cells were immediately seeded on pillars following the addition of F_{AB} CD45. F_{AB} regions were maintained in solution throughout imaging.

Cells were fixed and immunostained as previously described. Antibodies used in this section were used to target CD45 (Biolegend, 304019), phosphorylated Zap70 Tyr 319 (Cell Signaling, 2701S), phosphorylated Pyk2 Tyr 402 (Invitrogen, 44-618G), non-muscle Myosin IIA (Abcam, ab24762), Filamin A (Abcam, ab51217) and α-tubulin (Invitrogen, 322588).

Protein Inhibition. Latrunculin B, at a 1 μm concentration, was used to test the role of actin assembly in force generation. Likewise, the role of non-muscle Myosin IIA contractility was tested through the use of Blebbistatin (Sigma-Aldrich) at a concentration of 10 μm. The role of PI3K in mediating CD28-enhanced contractions was

tested by its inhibition with a wortmannin conjugate, wortmannin 17β-hydroxy analog [HWT]. HWT was preferentially used for selective PI3K inhibition over wortmannin due to its greater potency and specificity in targeting PI3K. To ensure that the role of PI3K assessed is downstream of CD28, rather than the TCR itself, we test HWT inhibition of PI3K in both the presence and absence of C28 costimulation. Akt, the downstream effector of PI3K that is thought to be responsible for initiating IL-2 secretion, is tested by inhibition via triciribine (Tric).

Data Acquisition. For tracking pillar displacements, timelapse stacks were bleach-corrected with a custom script for ImageJ and realigned via the StackReg plug-in developed by BIG at EPFL [79]. Pillar traces were then generated using the Particle Tracker plug-in developed by Mosaic at ETH [80]. Traces were then saved as text files, and imported into Matlab where background pillars were identified and cellular force measurements were calculated using a custom script. Relevant outputs that were collected include the average force per pillar, number of pillars in contact, and the total force per cell. An additional custom script was used to superimpose a vector map of the forces over the original timelapse video: to validate precise measurement of cellular forces.

3.4 Results

T cells exhibit multiple, discrete phases of engagement

Human CD4+ T cells seeded on micropillar arrays coated with activating antibodies were used to measure forces, schematized with the model below (Figure 3.1 A). T cell

behavior was qualitatively characterized and noted to exhibit a range of behaviors that could be roughly separated into discrete phases. Cells made contact with the top of the microarray in a manner similar to contact with a continuous surface, rapidly spreading after initial contact to cover numerous pillars (Figure 3.1 B1-2). This spreading process did not result in significant traction forces, suggesting that any future displacements were an active process and not the result of a change in the cell center of mass. After some time of stabilization, cells began to exert forces in an uncoordinated fashion, exhibiting individual pillar displacements that were unsynchronized in both magnitude and direction (Figure 3.1 B3). After a sustained period of uncoordinated displacements, which typically lasted in the range of five minutes to half an hour, cellular contractions slowly gained more uniformity, showing greater displacements along the periphery of the cell and largely being directed centripetally (Figure 3.1 B4). Once in this uniform contractile phase, abrupt changes in direction and magnitude mitigated, though total force exertion remained relatively constant. Cellular forces were measured throughout this process, during which the displacements of individual pillars were tracked and the relative forces exerted by the cell on them measured. Actively displaced pillars were distinguished from pillars not displaced by the cell through the identification of conserved movement across the entire system, which was comprised of minor perturbations in the stage and ambient drift. The forces exerted were calculated over time and used as a metric for calculating the force exerted by the cell (Figure 3.1 C). Forces exerted by T cells on micropillar arrays were calculated to be on the order of 58 (±22) $pN/\mu m^2$, with a total force of 1.23 (±0.36) nN per cell.

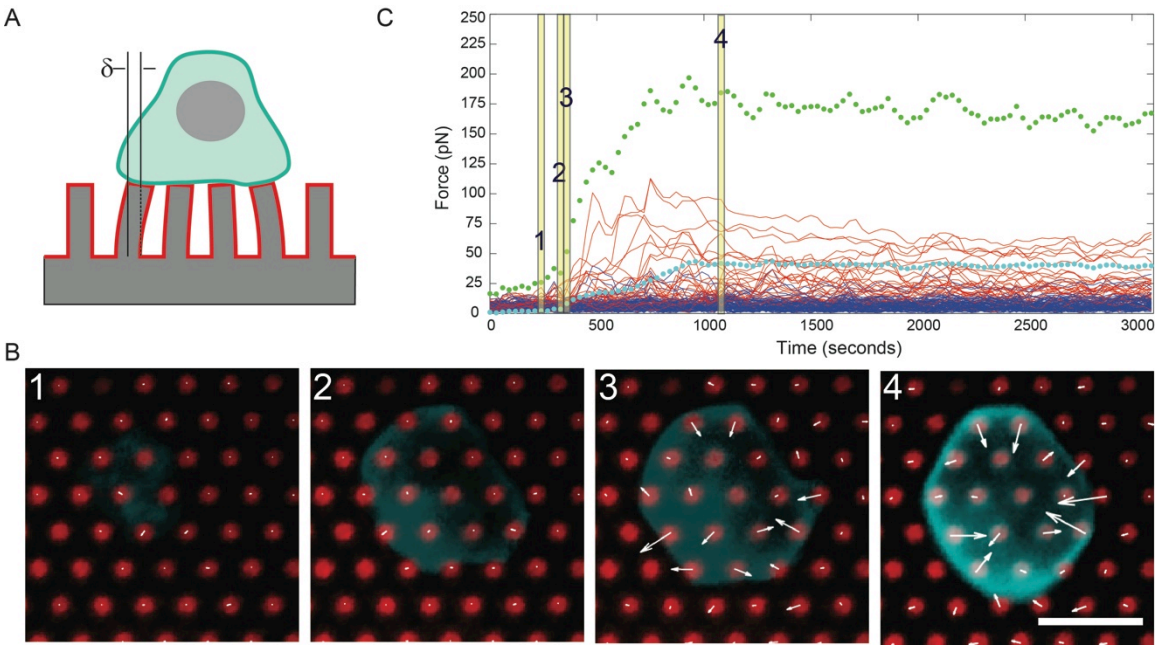

Figure 3.1. T cells exert forces on micropillar arrays (A) A 2D schematic shows the typical interaction of a T cell (blue) with the antibody-coated micropillar array (red). The displacement due to cellular exertion, δ, is used to calculate the force generated as described in Section 3.2. (B) Four time points that correspond to discrete phases are numbered and shown in (C). In (1), a cell as it first makes contact with the micropillar array. After initial contact, the cell rapidly spreads (2) while exhibiting minimal contractile force. Cells then initiate force generation on the micropillar array (3) by initially applying unsynchronized contractile forces, marked by white arrows. Finally, cells reach a stable equilibrium (4) where the greatest force exertion occurs along the cell periphery and are oriented towards the center of the cell. Scale bar in C4 denotes 5 μm. (C) A plot of T cell force exertion over time, where each solid trace represents an individual pillar. The blue traces are pillars that are not in contact with the cell, whose ambient movements are tracked and used to remove the contribution of ambient drift from forces generated. The red traces show the interactions of the cell with individual pillars. The dotted cyan line shows the average force exerted on each pillar by the cell, whereas the dotted green line represents the total force exerted by the cell, scaled by 5 so as not to skew the plot. The total force is measured once the net forces have stabilized (here, >1000 seconds).

T cell contractile forces are conserved across differing rigidities

To ensure that the forces measured were descriptive of cell behavior; contractile forces for cells on costimulated surfaces were measured on pillar arrays of differing effective Young's moduli. Pillar diameter was kept constant at 1 μm diameter, so as not to impact contact area, and T cell force generation was measured on pillars of varying heights of 3 to 9 μm. This approach has previously been used to demonstrate that epithelial cells maintain a constant displacement, rather than a constant force, when interacting with soft pillars of differing stiffness [81]. Pillars of heights 5, 6, 7 and 8 μm were all found to give reliable and consistent measurements. Below 5 μm, pillar displacements were too nominal to be measured precisely and at 9 μm, pillars were displaced to the extent that neighboring pillars would come in contact, making it difficult to accurately measure the total force involved in displacements. This behavior, where the degree of displacement varied with the stiffness, was a preliminary indication that displacements were not conserved in T cells. To ensure that forces were conserved, forces measurements were carried out on pillars of heights 5, 6, 7 and 8 μm, which respectively represent effective stiffnesses of 2.4, 1.4, 0.9 and 0.6 nN/μM. Forces generated by T cells were found to be conserved across this range (Figure 3.2 black). Moreover, cell spreading area was not found to be statistically different across these tested pillar heights (Figure 3.2 red). It is worth noting that these surfaces span a four-fold change in stiffness. Previous work that evaluated IL-2 secretion spanned a much wider range of stiffness, 3-5 orders of magnitude, and thus this conservation of force across micropillar heights does not discount that T cells can generate differential forces across a wider range of stiffness.

Thus, while this range may not be suitable for evaluating the effect of rigidity, the range tested here is appropriate to show that force generation, rather than pillar displacement, is a more appropriate metric for evaluating of T cell activation. This contrast in cellular

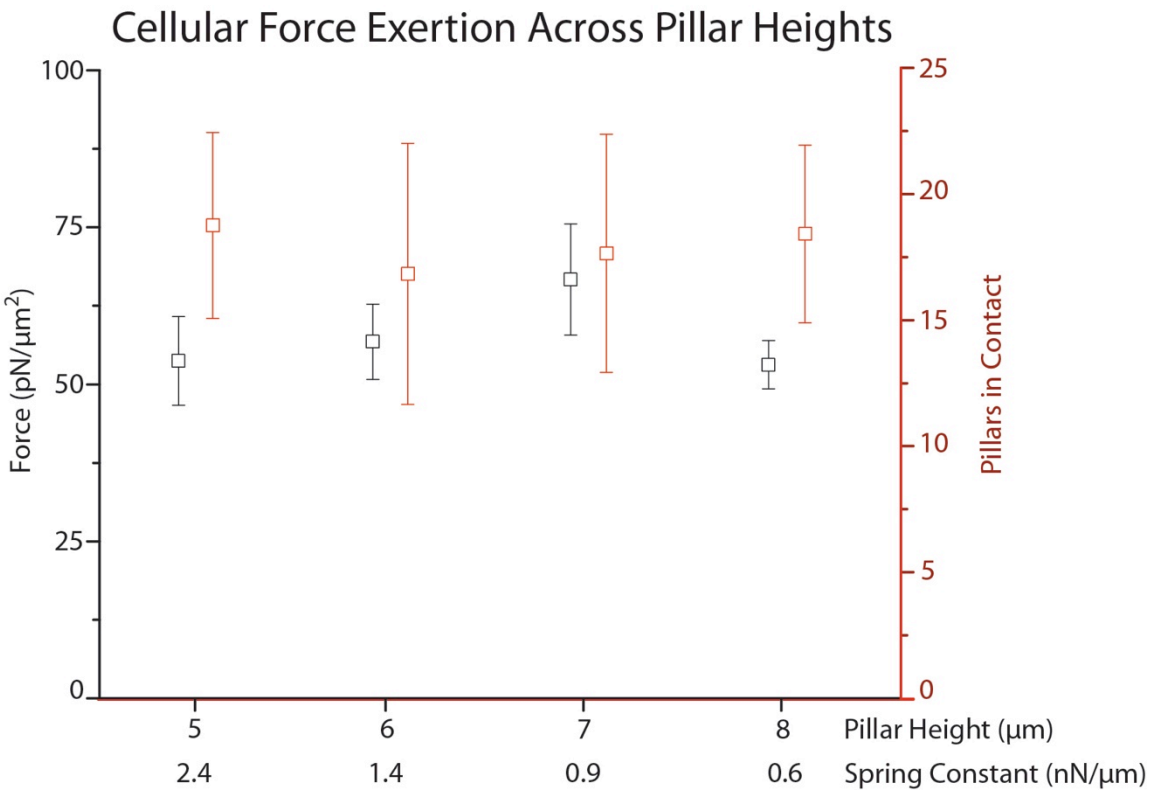

Figure 3.2. Cellular force exertion across pillar heights. T cell forces were measured across a range of pillar heights, 5-8 μm, that represent a four-fold change in stiffness. Force per area, indicated in black, was found to be consistent across this stiffness range. Likewise, the number of pillars that a cell was in contact with, indicated in red, was also conserved across this stiffness range, indicating that both force per area and total cellular force were conserved. Data is representative of >3 experimental runs. Means are plotted, with error bars representing the standard deviations for both force per area and pillars in contact.

behavior is suggestive of a different mechanism of generating and sustaining forces in T

cells than in epithelial cells.

To further characterize this behavior, we tested inhibition of the cytoskeletal network. Work highlighted in the previous chapter illustrated that the cytoskeleton played a significant role at the immune synapse and functioned in regulating protein diffusion. The role of the cytoskeleton in generating forces was tested here using the same approach of inhibiting F-actin assembly through LatB-based inhibition. LatB was effective at abrogating cellular forces, demonstrating that in addition to being responsible for regulating lateral diffusion along the membrane, the cytoskeleton is critical in generating cellular forces. To see whether force generation relied on myosin activity, non-muscle Myosin IIA contractility was inhibited through the application of blebbistatin. Blebbistatin functions by impairing Myosin ATPase activity and thus prevents myosin-induced force generation. Blebbistatin treatment of cells also led to abrogation of cellular forces, indicating that both actin and myosin, though likely a combination of actomyosin contractility, leads to T cell force exertion on micropillars. Staining for cytoskeletal constituents show enrichment of F-actin at the points of contact with the micropillars, whereas Myosin IIA showed moderate depletion from these regions (Figure 3.3 A). Previous work in the direction of understanding the molecular pathways involved in the generation of contractile forces has relied on loss-of-function point mutations [82]. The relative depletion of Myosin IIA from the regions of contact was somewhat unexpected. The significance of this displacement from the site of force exertion is not fully understood, but may be rationalized in the context of the functional distance needed to induce myosin contractility. Non-muscle Myosin IIA functions in multiple capacities,

including cellular protrusions, adhesion disassembly and nuclear relocalization [82]. These numerous roles occlude the resolution needed to make a more definitive assertion on the displacement of Myosin IIA from the contact regions of cellular contact with micropillars.

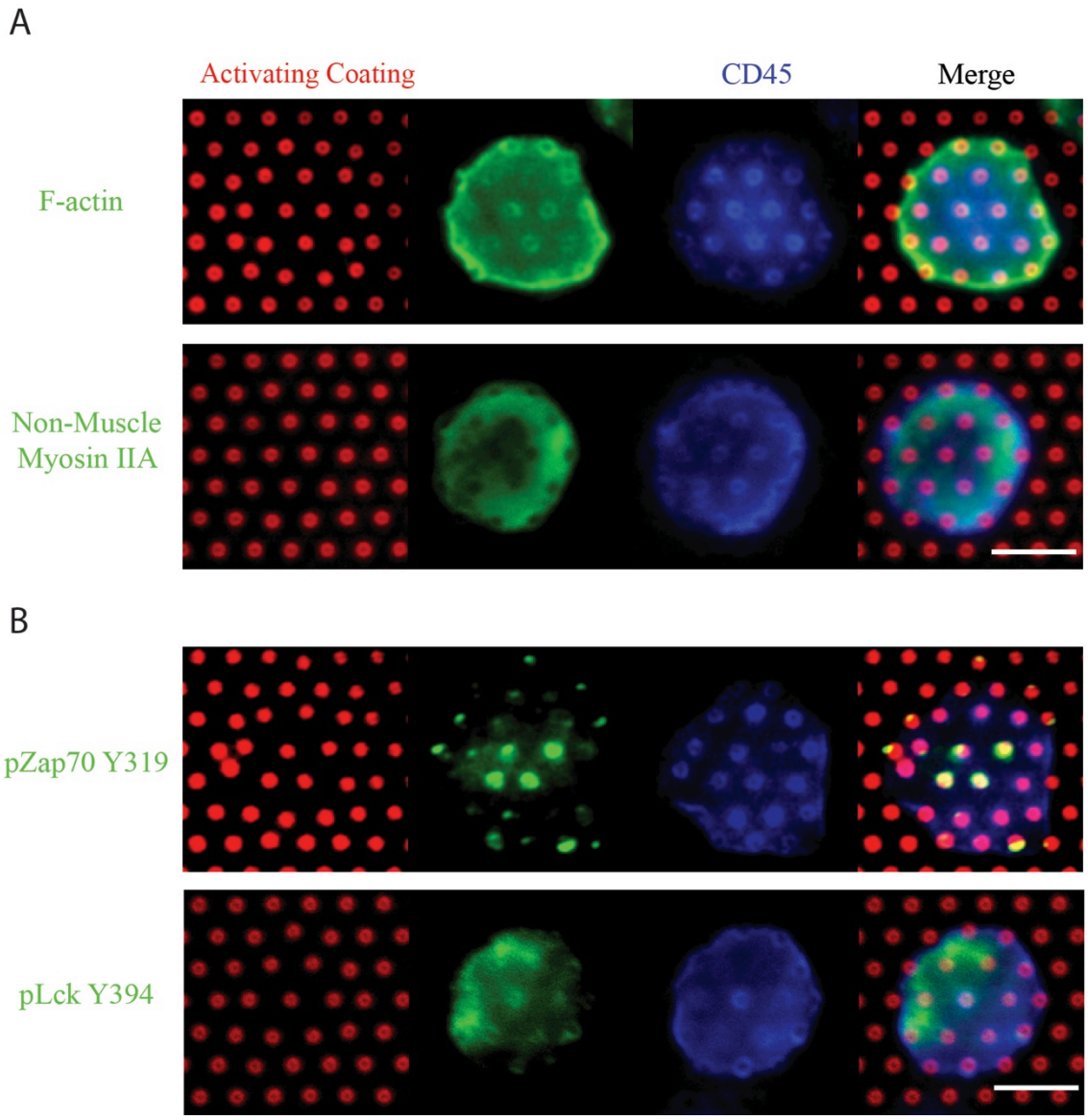

Figure 3.3. Protein enrichment on micropillars. (A) Cytoskeletal constituents F-actin (top, green) and non-muscle Myosin IIA (bottom, green) are stained for in T cells seeded on micropillar arrays. The activating coating, antibodies that activate CD3ε and CD28 (red) is imaged at the interface of the top of the

micropillars with the T cell. (B) The active forms of activating factors Zap70 and Lck are stained for. Scale bars denote 5 μm.

Having established that the fundamental components were in place for force generation, we next looked to ensure that T cells were being activated, and thus the noted forces were a response to cellular activation. The active, phosphorylated populations of Lck (Y394) and Zap70 (Y319) were stained for determine cellular activation; the active form of Lck has been covered in depth in the previous chapter. The active form of Zap70 is used as a proxy for TCR triggering, its phosphorylation both following and being dependent upon Lck activity at the TCR [73, 83]. Both Zap70 and Lck showed substantial enrichment at the regions of the cell interface in contact with micropillars, suggesting that activation through the TCR had been initiated (Figure 3.3 B). In the previous chapter, we describe a mechanism for the integration of CD28-mediated costimulation with the TCR pathway. The remainder of this chapter builds on the role of costimulation, and looks at the contribution of CD28 in the context of cellular forces.

Costimulation through CD28 enhances T cell contractile forces

The force measurements taken so far describe the effects of cellular activation when both TCR and CD28 are engaged. To measure the impact of CD28 triggering on force generation, we compared force generation on surfaces that triggered TCR activation, both in the presence and absence of CD28 triggering. Forces were measured using the pillar aspect ratios that were previously described and revealed that the inclusion of CD28 costimulation increased contractile forces from 0.70 nN to 1.26 nN per cell: an increase

of over 80% (Figure 3.4). Neither cell spreading area nor the number of pillars interacted with were observed to differ due to CD28 activation. As discussed earlier, CD28 costimulation modulates a wide range of factors, including increasing the sensitivity of a

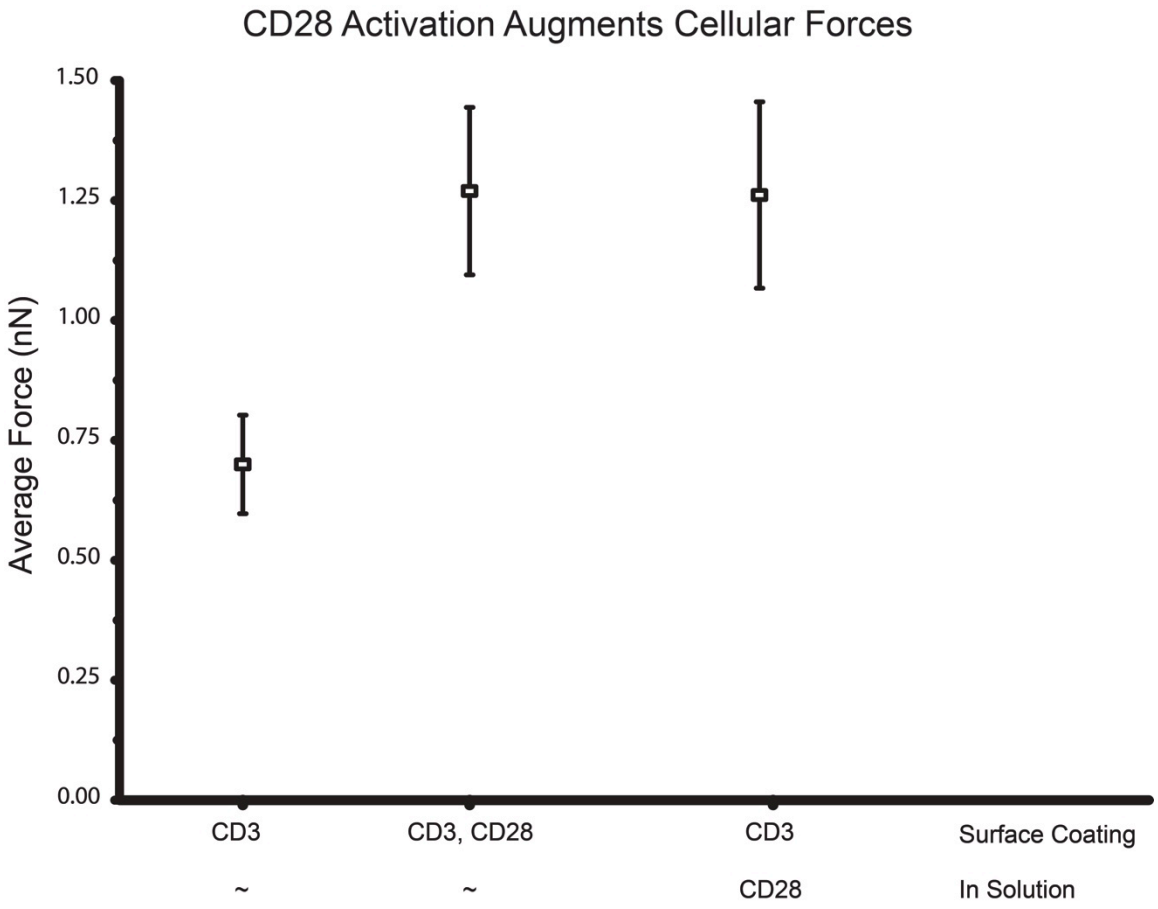

Figure 3.4. CD28 activation augments cellular forces. This graph describes the role of CD28 in mediating TCR forces. Inclusion of CD28 activation, either on the coating surface or in solution, equally increases T cell contractile forces. Forces measured here represent the total force exerted by a cell through micropillars. Pillar contact area is not augmented by the inclusion of CD28, either in solution or on the surface, and thus total cell force is proportional to force per area.

T cell to antigen engagement, inducing a greater rate of proliferation and a significant increase in IL-2 secretion. However, the capacity of costimulation to modulate cellular forces has not been previously described. We anticipate that this augmentation of cellular forces is facilitating one or more of these other processes. To resolve the role of this increase in activation forces, we next characterized the pathway through which CD28 acts to augment force generation.

CD28 triggers IS mechanoresponse, but is not mechanosensitive

To better characterize the mechanism involved in CD28 modulation of cellular forces, we next assess the capacity CD28 acts as a mechanosensitive receptor; testing for mechanosensitivity requires a method of differentially targeting the TCR and CD28. CD28-based costimulation was relocalized from surface presentation in parallel with TCR stimulation, where the underlying rigidity of the substrate would be responsible for a mechanoresponse, to in-solution targeting of CD28, where the strength of the interaction would rely only on antibody binding affinity. After initial coating of micropillar arrays with TCR-activating antibodies, residual binding sites on the surface were blocked with 4% BSA for one hour. Cells were then seeded with activating antibodies to CD28 introduced in-solution, permitting interaction of the antibody with CD28 in a manner independent of surface properties. Delineating the presentation of CD28 from on the micropillar array with CD3 targeting antibodies to in solution did not show a notable change in force exertion or behavior (Figure 3.4). That the two methods of CD28 activation were equally effective suggests that while costimulation was a mechanoresponsive process, the CD28 receptor was not the key mechanosensitive

mediator of the response. Rather, an internal mechanism for increasing contractile forces was likely responsible for the change.

CD28 activation differentially augments protein enrichment

The process of activation-induced force generation was previously found to be fully dependent on cytoskeletal activity; inhibition of either actin or non-muscle myosin IIA both led to abrogation of cellular forces. This was true in both the presence and absence of CD28 activation, inclining us to postulate that the CD28-mediated mechanoresponse also required the activity of these two cytoskeletal components. Costimulation has been shown to stabilize membrane condensation at sites of TCR activation, leading us to look at constituents that were known to preferentially associate with CD28 over the TCR [84].

We first looked to measure whether CD28 impacted TCR triggering. Activation of CD28 either through surface presentation or in solution both showed comparable levels of phospho-Zap70 localization, suggesting a mechanism downstream of Zap70 recruitment to the TCR and likely downstream of CD28. In keeping with this theme of mechanoresponse, we quantified the relative enrichment of key cytoskeletal components at the pillar array (Figure 3.5). F-actin was seen to increase with the incorporation of CD28 activity: in agreement with an increase in contractile forces and LatB-based inhibition of F-actin abrogating cellular forces. Interestingly, the behavior of myosin IIA was unchanged; rather Filamin A was modulated by CD28 costimulation. Filamin A was notably depleted from the sites in contact with the pillars, which we found somewhat

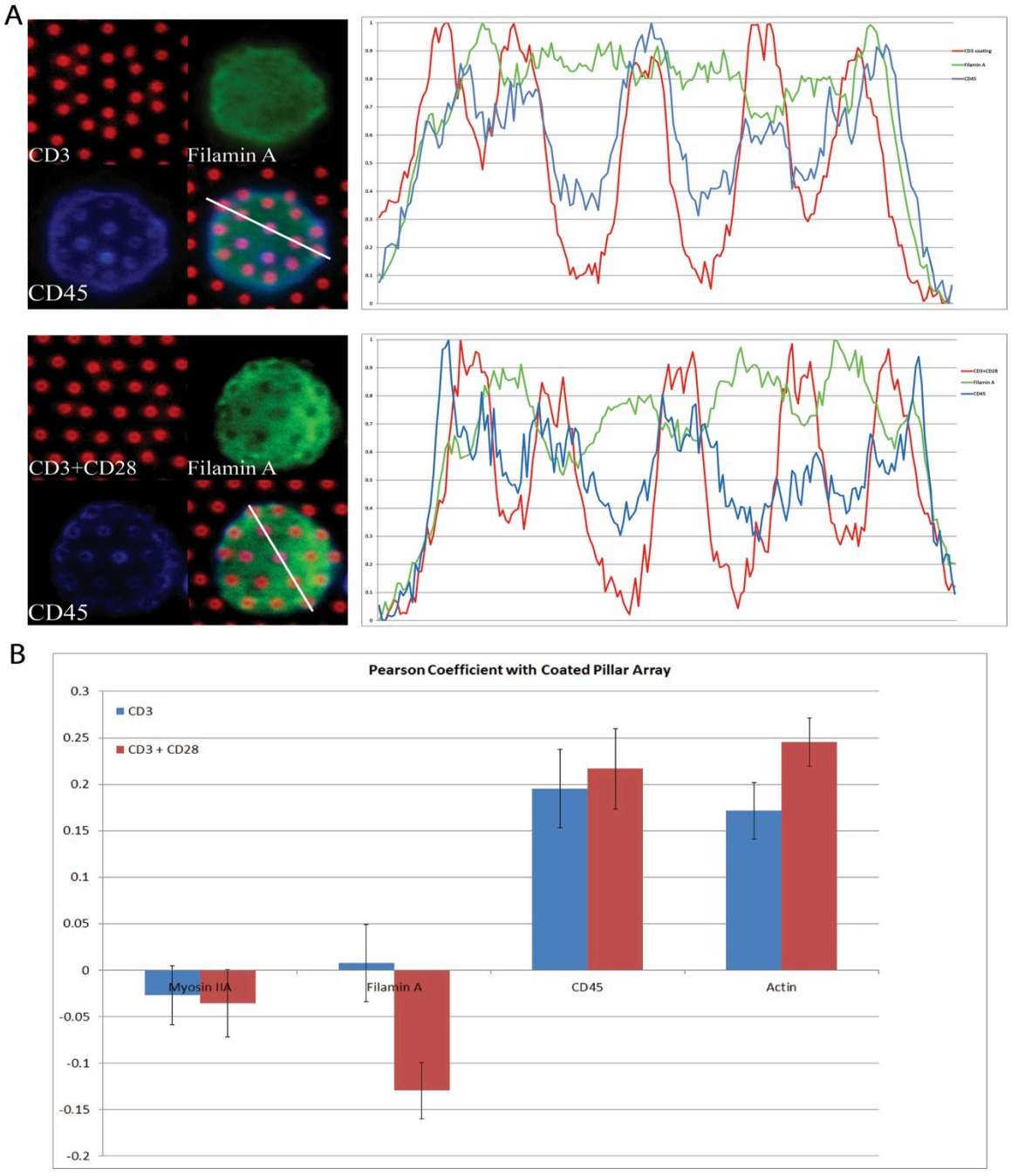

Figure 3.5. CD28 modulates cytoskeletal enrichment. (A) Filamin A did not show preferential localization on micropillars when the TCR was triggered (top). However, Filamin A was depleted from micropillars, in a manner similar to Myosin IIA, when CD28 was added to the surface coating (bottom). The relative intensities of pillar surface coating, Filamin A and CD45 are tracked along the white line in the Merged figures, and the distribution of protein is shown on the right. (B) The effect of CD28 activation was measured on Myosin IIA, Filamin A, CD45 and F-actin by Pearson correlation. Whereas Myosin IIA

distribution was unaffected by the inclusion of CD28 activation, Filamin A showed a negative colocalization with the micropillars, indicated by a Pearson value less than 0. Moreover, while CD45 was unperturbed, F-actin showed increased localization to micropillars in the presence of CD28.

perplexing given a known linkage between Filamin A and CD28. These results achieved through immunostaining yield additional insight into the physical manipulations through which increased forces may be generated. However, they do not describe the pathway through which CD28 signaling triggers increased contractile forces. Filamin A is a compelling candidate for this role, as it does bind directly to CD28 and links to the actin cytoskeleton. Though, the relative depletion of Filamin A from sites of CD28 engagement suggests that its predominant role in this process is not through direct linkage with CD28. Thus far we have shown that CD28 is mechanoresponsive but not mechanosensitive, indicating that there is a downstream pathway to mediate this mechanoresponse. We next looked to PI3 kinases that, like Filamin A, interact directly with CD28 but also have a well-characterized pathway and available chemical methods of manipulation.

PI3K relays CD28-mediated contractility

Phosphatidylinositol 3-kinase [PI3K] directly associates with the YMNM motif on the cytosolic tail of CD28, helping propagate costimulation and making for a compelling mediator for relaying changes in contractile forces [39, 85, 86]. The PI3K pathway is a major though not exclusive intermediary for CD28 costimulation. Its roles include Akt and PDK1 recruitment through D3 lipid production, PKCθ recruitment to the immune synapse and Akt phosphorylation [85, 87, 88]. Previous work has shown that disrupting

the PI3K interaction to CD28 via a mutation of the binding site does not impair IL-2 secretion, unlike a disruption in the Src-kinase binding PYAP domain of CD28 [89].

Inhibition of PI3K was achieved using a wortmannin conjugate, 17β-Hydroxywortmannin [HWT], which was used for its higher selectivity for PI3K. As a secondary target, wortmannin binds and inhibits mammalian target of rapamycin [mTOR], which plays an active role downstream of PI3K. Numerous proteins within this pathway are considering key targets in the dissemination of cancer [90]. Cells were seeded on micropillars and given 15 minutes to initiate contact. HWT was subsequently washed-in at a concentration of 50 nM and contractile forces were measured. On costimulatory surfaces, contractile forces were reduced to 0.82 (+/- 0.06) nN as a result of treatment with HWT (Figure 3.6). To ensure that PI3K inhibition by HWT was directly affecting costimulation, and not instead responsible for forces generated through TCR-based activation, we subsequently applied HWT to cells activated exclusively through the TCR. TCR-dependent force generation was unaffected by HWT inhibition, generating forces of 0.69 (+/- 0.07) nN, suggesting PI3K plays a role in mediating a CD28 mechanoresponse (Figure 3.6). We next looked at a downstream target of PI3K, Akt, whose role in costimulation is tied to long-term IL-2 production. Inhibition of Akt via triciribine, using a post-adhesion wash-in method as previously described, did not impact cellular forces generated on costimulatory surfaces (1.29 +/- 0.11 nN), suggesting that though Akt directs long-term IL-2 secretion, it does not play a role in generating cellular forces during the first hour of activation (Figure 3.6).

Finally we targeted PDK1 which plays a significant role in triggering a number of

downstream protein kinases [91]. Though much effort has gone into identifying selective inhibitors of PDK1 for targeting cancer metastasis, few candidates have been identified. The novel inhibitor GSK 2334470 [GSK] has been touted as highly selective [92-94]. We tested the effects of PDK1 inhibition with GSK at a concentration of 10 nM. Within 15 minutes of GSK wash-in, cells abated contractile forces in a manner similar to what was previously observed with LatB treatment of contractile cells. Together, selective inhibition of PI3K and PDK1 suggest that while PDK1 is critical for forces generated through the TCR and CD28, the role of PI3K is to integrate CD28 costimulation.

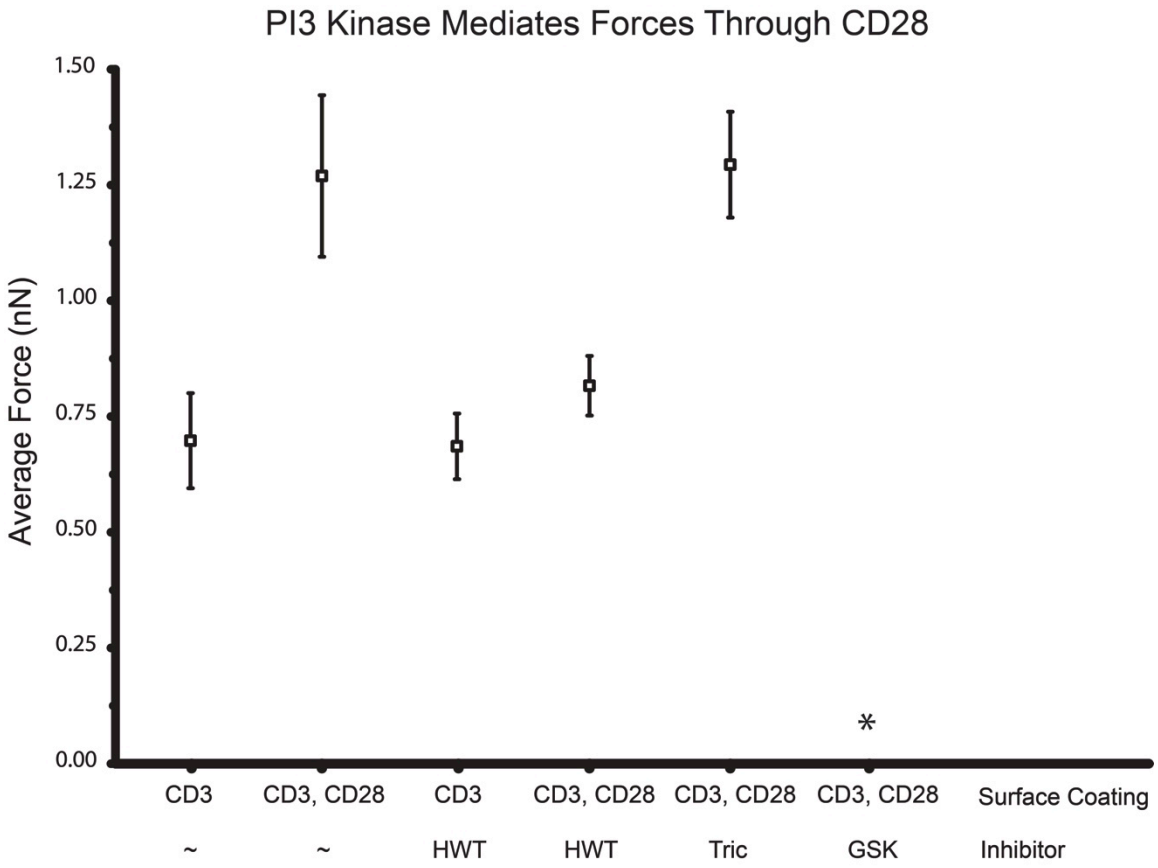

Figure 3.6. PI3 Kinase mediates forces through CD28. CD28-dependent contractile forces were tested by selective inhibition of its downstream pathway. PI3 kinases were inhibiting using the more selective wortmannin conjugate 17β-Hydroxywortmannin (HWT), which mitigated the contractile forces generated

through CD28 but had no effect on cells activated through CD3 alone. Inhibition of Akt, which is further downstream of PI3 kinase, with Triciribine (Tric) has no effect on cellular force generation. Inhibition of PDK1 with the novel inhibitor GSK 2334470 (GSK) abrogated cellular forces entirely, which is denoted by an asterisk (*).

3.5 Discussion

The results in this chapter highlight a number of key findings. First, it highlights and demarcates the mechanoresponsive role of CD28 in IS dynamics. CD28 is known to dramatically influence T cell response through a number of intermediates, leading to substantial ramifications on T cell fate and function. We demonstrate here that CD28 relies on its downstream constituent PI3K to convey modulation of mechanical forces independent of TCR-triggered force generation. Though Akt is downstream of PI3K activity, it does not contribute to force generation. PDK1, however, plays an essential role in TCR-mediated contractile forces. A number of proteins probed in these experiments show preferential localization, some uniquely through CD28 such as Filamin A, and others more broadly. Future work will look to further characterize this preferential localization with the interest of developing a model for force generation. Importantly, this work will also seek to resolve how PDK1 loops back to the cytoskeletal network.

The work in this chapter demonstrates that changes in contractile forces during T cell activation can be captured and accurately measured through the use of micropillar arrays: providing micron resolution on cellular forces. This is not the first instance of complex topologies being used to explore T cell activation, though we anticipate that the findings presented above will facilitate future efforts to identify how cellular forces are

coordinated with T cell activation. We consider both the mechanism of force generation through the IS as well as the role of the CD28 in the process to be compelling. It is worth noting some aspects of CD28 behavior during costimulation, which may illuminate its role in mechanoresponse. Following CD28 engagement, it is endocytosed in a clathrin-dependent fashion through the coordinated efforts of PI3K and a number of proteins associated with vesicle formation and the cytoskeleton. The significance of CD28 endocytosis in the context of costimulation is still an unresolved question. CD28 is the sole costimulatory ligand to be constitutively expressed on the surface of a T cell, though its presence on the surface does recede as the cell matures. Whether this endocytotic behavior correlates with increased cellular forces remains to be tested. The work in this chapter does not exclude this prospect, which would be in keeping to the observed global mechanism of increased contractile forces upon CD28 stimulation.

Chapter 4 – T Cell Activation Demonstrates Multiphasic Behavior

4.1 Abstract

In this chapter, we employ a number of techniques to characterize changes in T cell behavior that are triggered by cellular activation. Micropillar arrays are again employed, though here they are used to capture morphological changes following the first hour that was the focus of the previous chapter. After exerting contractile forces for roughly the first hour, T cells manifest an invasive morphology, where they relocalize from the top to the base of the pillar array. Cells that have relocalized to the base of micropillar arrays are capable of producing IL-2, indicating that they are still undergoing activation. T cell invasion is also shown to coordinate with MTOC and phospho Zap70 Y319 relocalization, providing further evidence that T cell invasion does not preclude their activation. In concert with T cell relocalization, there is also substantial cytoskeletal reorientation and the redistribution of focal adhesion proteins. Finally, the motivation for the change in T cell morphology is examined, and through use of selectively coated cellular trenches, the formation of filopedia-like protrusions is found to be triggered by TCR activation. Activating cells probe these nonactivating regions through filopedial protrusions, but do not fully enter these trenches that lack TCR activation. Finally we look to put the forces and behavior of T cells observed in this and the past chapter in context. This is executed by assessing the mechanical properties of bone marrow-derived dendritic cells [bmDC]: one of the most proficient APCs at activating CD4 and CD8 T cells.

4.2 Introduction

Upon maturation, the roles of a T cell include the monitoring of peripheral tissues by identifying and responding to the specific antigen that it has been primed to target. However, the ability of T cells to monitor these regions relies on their ability to access peripheral tissues that are remote to the vascular system. The walls that line vascular structures are densely packed with multiple endothelial layers, the function of which is intended to maintain fluid pressure and flow. This function would be compromised by cell-size gaps that would facilitate immune cell passage. Rather than the vasculature containing such gaps, it is more rationale to postulate that lymphocytes utilize a unique process of passing vascular structures with minimal structural damage. There currently is a compelling model that demonstrates a stepwise process through which T cells transmigrate past tissue layers to enter peripheral tissues [95, 96]. These tissue layers are not homogenous, and are often composed of different cell subpopulations with varying differential receptor expression and mechanical properties. Collectively, these requirements indicate that T cells are hardwired to penetrate through a number of discrete tissue layers: a feat that is anticipated to take a greater force and plasticity than what was measured during IS formation in the previous chapter.

The previous two chapters focused on the process of IS formation and maturation: identifying key pathway components that modulate costimulation. Other research groups have also looked at ways to study the processes and significance of the IS. One approach to studying the IS has involved demarcating temporal phases of IS formation by changes in spatial protein localization at the interface [23, 67]. The benefit of such an approach is

that IS cues often follow such a temporal timecourse: where there are key events that must take place before the IS can mature to the next temporal phase. Others have instead attempted to integrate the behavior of the activating APC with that of the T cell: focusing on one or two key protein interactions and their direct downstream events [41, 97]. The aim of this chapter is to further characterize the interaction of a T cell with its activating surface, utilizing some features of these two models. In the previous chapter, we highlight the use of micropillar arrays in capturing cellular forces. During this early phase of cellular contractility on a costimulatory surface, T cells rest on the top of the micropillar while exerting contractile forces. In this chapter, we look at the long-term behavior of T cell on costimulatory micropillars, where they demonstrate the capacity to recognize and respond to the complex topology that these micropillars provide: leading to migration into the micropillars towards the base of the array.

4.3 Materials and Methods

Fabrication and Substrate Preparation. In addition to the micropillar masters that were previously described, masters for cell trenches were also employed. Work with bmDCs, which exhibit greater contractile forces than T cells, necessitated fabrication of 1 by 4 μm micropillars. The fabrication process was similar, and made use of 1μm μPG101 Heidelberg laser writer to directly pattern SU-8 2005 photoresist.

The same approach was used in the fabrication of cellular trenches. Positive molds were fabricated with laser lithography to be 1 μm in diameter and 5 μm deep. Negative molds were cast in PDMS (Sylgard 184, Dow Corning) from these masters, silanized overnight

with (tridecafluoro-1,1,2,2,-tetrahydrooctyl)-1-trichlorosilane (United Chemical Technologies) and then used to cast trenches directly onto thickness #0 Fisherbrand glass coverslips that were cleaned as described previously.

Cell Isolation and Culturing. Resting peripheral human CD4+ T cells were isolated and enriched from whole blood as previously described. Immature mouse bone-marrow derived dendritic cells [bmDC]s were isolated by Subhashini Srivatsan (Shaw lab, Washington University in St. Louis) from mouse bone marrow following standard protocol [98, 99]. These cells were then matured for 6-8 days using RPMI-1640 media supplemented with 10% Hyclone serum and 2% Granulocyte-Macrophage Colony-Stimulating Factor [GM-CSF], at which point they were seeded on fibronectin-coated micropillar arrays. Force generation was then measured as described in the previous chapters.

Antibodies and immunostaining. Cell fixation, permeabilization and immunostaining were all performed as previously described. For comparisons of contractile cells with invasive cells, time points where the three phases manifested were used to directly compare protein localization. The ideal timepoint for capturing the three phases was heuristically determined to be at 3 hours. The behavior of contractile cells at 3 hours was compared to their behavior during the first hour and was not found to be substantially different.

Characterization of cell behavior on micropillars. Cell behavior was characterized by

intermittent imaging of cells maintained at 37°C and 5% CO_2 rather than tracking the behavior of one field of view over time. This was done to ensure that a large fraction of the population was captured. Three runs were performed using both TCR activating surfaces and TCR-CD28 activating surfaces, each with at least 50 timepoints. The inclusion of CD28 was not found to augment cell behavior over time.

IL-2 secretion and statistical analysis. IL-2 capture and quantification was performed using the methodology described in Chapter 2. Here however, secretion was measured from 12 to 13 hours, rather than from 6 to 7 hours. The motivation for this deviation was to ensure that the majority of cells had entered the invasive phase, which occurs after the initial 8 hours of activation. Experiments were repeated threefold and statistical analysis was performed as previously described.

4.4 Results

T cells exhibit temporally-coordinated phases on 3D substrates

T cells were captured exerting a dynamic range of forces during the half hour of activation on micropillar arrays. By the end of this half hour, a majority of T cells were found to still be contractile, but no longer dynamically exerting forces on the substrate.

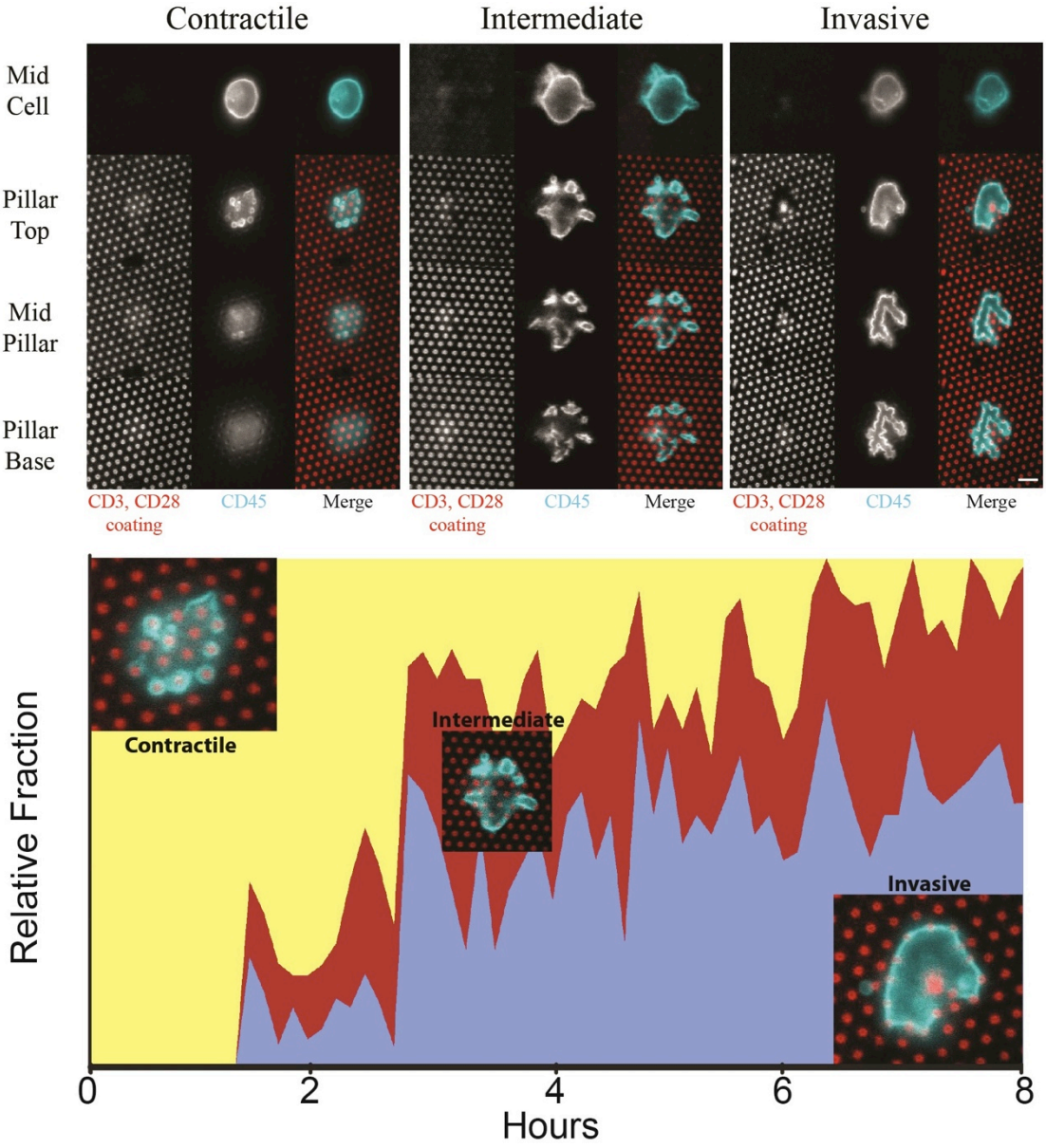

Figure 4.1. T cell morphology over time. (A) T cells exhibit multiple distinct phases on activating micropillars. The initial contractile behavior where force measurements are taken (left) is later replaced by an intermediate phenotype (middle), where cells extend filopedial projections to interface with the surface. After some time, cells fully relocalize to the base of the array (right):, exhibiting an invasive phenotype. Scalebar represents 5 μm. (B) Tracking cell behavior and classifying them into these three phases over time shows that the majority of cells exit the contractile phase by 8 hours following initial activation. Scale bars denote 5 μm. Temporal tracking fractions are a weighted average of three experiments.

We next looked to characterize whether cells in this contractile phase could maintain cellular activation, and thus were stable, or if dynamic force exertion would again resume. Following a prolonged period of stagnancy, cells began to exert filopedia-like protrusions that were observed extending both parallel to and protruding into the micropillar array. Over time, these protrusions stabilized as they made contact with the base of the array. As time progressed, T cells relocalized from the top of the pillars to the base of the array, eventually centralizing their contact and aligning to the base of the array. This relocalization was tracking through timelapse and three distinct phases were identified (Figure 4.1 A). During the first hour of cellular activation, T cells exert contractile forces on the top of the array. T cells then extend filopedia-like protrusions in an intermediate phenotype where the cell is monitoring its environment and while predominantly on the top of the micropillars, they may make contact with the base of the array. In many cell types, this monitoring behavior is tasked to the cilia; however, primary cilia have not been identified in lymphocytes, though these filopedial protrusions seem to serve a similar role [100-102]. Once these filopedia made contact to the base of the array, the cell began to migrate to the base of the array, in a phenotype described as invasive. Unlike the previous contractile phase, where forces were displaced towards the central region of the cell, invasive protrusions displaced pillars away from the cell's center of mass. This change in direction was taken to be indicative of, and later correlated to, the relocalization of the cell to the base of the array. Quantification of the forces needed for this process was not feasible with our current set-up. Contractile forces have so far been calculated using a modification of the cantilever equation, in which one of the

underlying assumptions is that forces are exerted at a specified known height. For invasive cells, where there is extensive contact between the cell and the sides of the pillar, there is no direct method for assessing the distribution of force. Nor can it be assumed that forces are equally distributed along this region of contact.

It is evident that greater forces are required to fully displace micropillars for cellular invasion. However, the extent of this difference in force generation is not directly measured. Rather, we apply a qualitative analysis of cellular behavior by classifying cells into these three phases, contractile, intermediate and invasive, and assess the progress through these phases over time. Quantification of cellular phases over time showed that by three hours, roughly half of the cells had stopped exerting contractile forces on the top of the pillar array and had either proceeded to an intermediate or invasive phenotype (Figure 4.1 B). By six hours, the majority of cells had proceeded to an intermediate or invasive phenotype with roughly half in each of these two phases. The time-dependent migration of T cells into micropillar arrays was unexpected. The sensitive state of pre-activated T cells, where failure to successfully form an IS and activate results in anergy and prompts cell death, led us to subsequently access whether these invasive cells were successfully activating.

Cellular Invasion Impacts Activation

Previously we identified protein localization in cells exerting contractile forces on micropillars. The relocalization of proteins critical to costimulation, the active forms of Zap70 and Lck, suggested that contractile cells were capable of initiating cellular

activation. However, the relocalization of the cell following the initial contractile phase led us to question whether invasive cells were in a state that could be considered

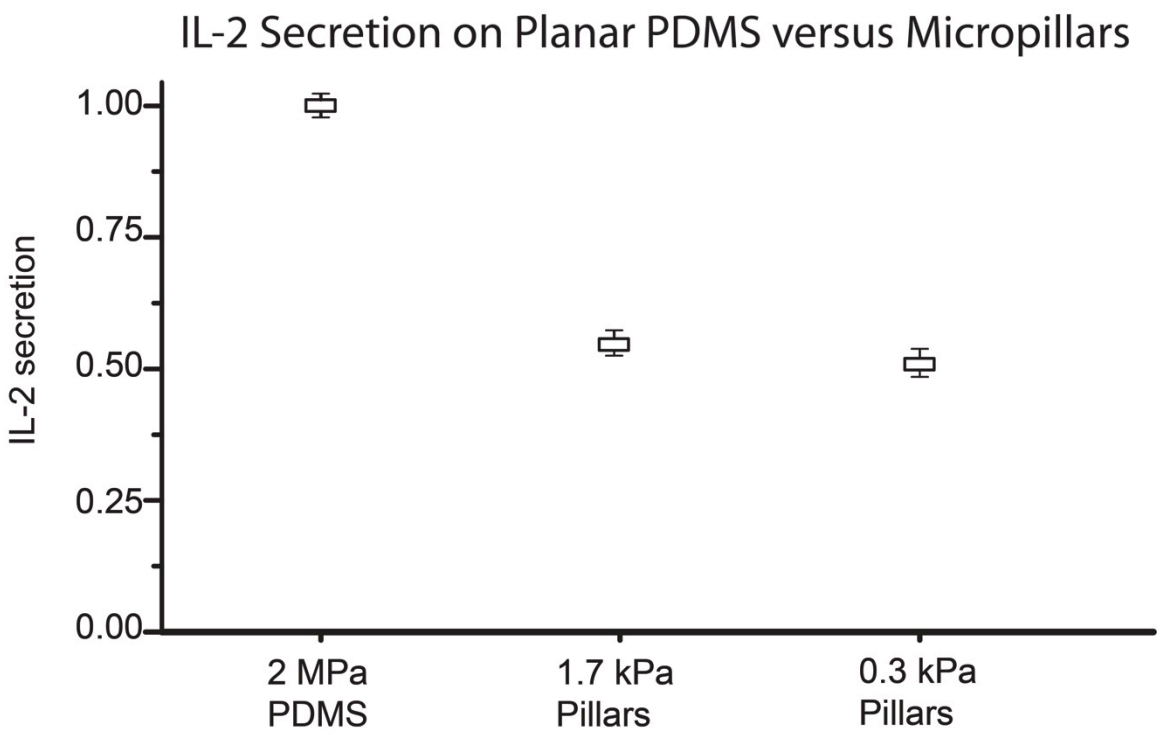

Figure 4.2. Invasive cells are activated. IL-2 measurements from 12 to 13 hours after seeding demonstrate that invasive cells are capable of secreting IL-2. The level of secretion was comparable between micropillars of 1.7 kPa (5μm) and 0.3 kPa (9 μm), though both secreted roughly one half of adjacent cells that spread on regions of planar PDMS (2 MPa stiffness).

activating. In addition to substantial structural reorganization, T cells physically contort their shape in an effort to make contract with the base of the array. T cell activation *in vivo* is predicated by the successful interaction of a T cell with an activating APC. Howerever it is unlikely for such an interaction to form and sustain for the desired timeframe without assistance. One of the roles of high endothelial venules [HEV] within

the lymph node is to facilitate this T cell-APC interaction [103-105]. T cells enter HEVs through a multistep process similar to what is observed with their invasion into micropillars. The majority of T cells on micropillars had exited the contractile phase by eight hours, so we looked to measure the ability of T cells to secrete IL-2 after this time point. One hour IL-2 secretion was measured, as previously described, by indirect capture at 12 hours: sufficient time to ensure cellular invasion. IL-2 of invasive cells was measured and compared to cells activating on the planar PDMS regions adjacent to the micropillars. These planar regions were an ideal internal control as all temporal, cell quality and protein level factors were identical except for the changes introduced by the micropillars. Additionally, we measured the effect on IL-2 secretion of both 5 μm and 9 μm micropillars, to resolve whether the effective stiffness of the micropillars may account for a difference in cellular activation. Though no difference was noted between 5 μm and 9 μm micropillars, both demonstrated roughly half the level of secretion as adjacent cells that were activating on planar PDMS (Figure 4.2). The noted reduction in IL-2 induced by the micropillars may be accounted for by a number of factors. It is possible that the process of relocalizing to the base of the microarray delays activation processes and thus the level of cytokine production is representative of a cell that has spent less time activating. This would indicate a delay in an interm process, as early indicators pointed to the initial triggering of the TCR and CD28 receptors. Alternatively, the micropillars may augment the activation process during the first hour, possibly through a change in the effective stiffness or due to the discontinuity of the activating surface. There is strong precedent, both from the perspective of T cell differentiation and for the development of other cell types, where early programming can have a profound

effect on long-term differentiation [106-111]. Cells that invaded into micropillars were found to still be capable of dividing on roughly the same timescale as those on planar surfaces, with the majority of cells undergoing mitosis 35-40 hours following initial activation. Collectively, these results suggest that cellular activation is initiated on micropillars and T cells later proceed through division, indicating successful programming by artificial APC.

Phase change coordinates with protein relocalization

To further resolve whether there was delayed or impaired activation of cells that had invaded into micropillars, we considered a number of critical IS maturation steps. Two discrete intermediate events that are required for IL-2 production, our metric of choice, is MTOC relocalization to the activating surface and NF-κB nuclearization. Microtubules are credited for a number of general tasks ranging from the retention of cellular structure, polarization of effector molecules, receptor endocytosis and maintenance of actin-dependent structures [65]. Specific to IS maturation, the microtubule organizing center [MTOC], a morphologically distinct site of microtubule nucleation, plays a critical role during the activation of T cells by APCs. During activation, the MTOC relocalizes from the uropod to the cell-surface interface within minutes of sustained contact, from where it facilitates in the activation cascade pathways [112]. This process occurs soon after IS formation, generally within the first five minutes of adhesion, and is observed when T cells are activated by either APCs and by planar artificial substrates: making it an ideal candidate for an interim IS maturation metric. NF-κB translocation to the nucleus occurs later during IS maturation. Upon translocation to the nucleus, NF-κB stabilizes IL-2

mRNA, promoting its production and subsequent secretion, making it another strong candidate for an interim, though somewhat later, maturation metric [87, 113, 114].

T cells were immunostained to assess whether there was MTOC relocalization at 15 minutes on both TCR-activating and costimulatory surfaces. This staining revealed that the MTOC failed to localize to the cell interface on the expected timescale (Figure 4.3, left). As shown in the previous chapter, however, the active forms of both Zap70 and Lck did localize to the regions of costimulation during this scale (Figure 3.3). Rather than repositioning within minutes as occurs on planar surfaces, less than 10% of the cells

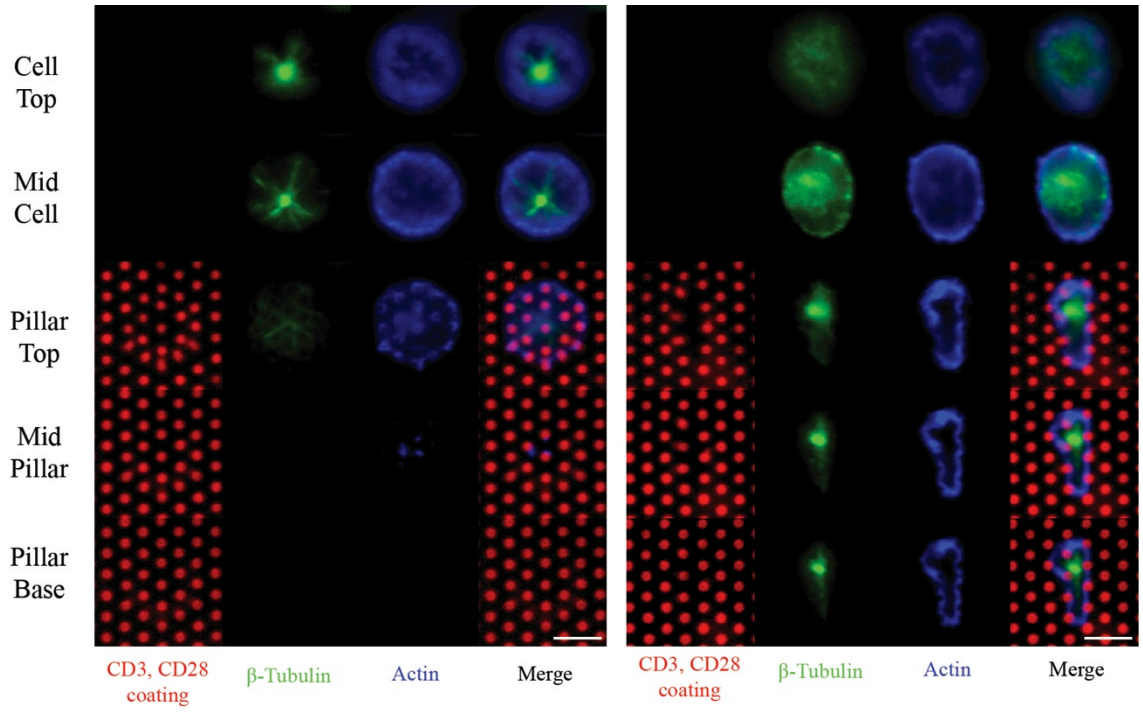

Figure 4.3. The position of the MTOC is tracked and found to be coordinated with the movement of the T cell to the base of the array by staining for β-Tubulin (green). In contractile cells (left) the MTOC delays in its movement to the site of activation, and is located in the region between the mid and upper cell. In invasive cells (right) the MTOC relocalizes to the base of the array, and is located between the pillar base and mid pillar. White scale bar denotes 5 μm. Change in *Z* height from level to level is roughly 3 μm.

exhibited a relocalized MTOC after initial contact. Our previous work indicated that cellular invasion was initiated following the first hour of contractile behavior. Fixing cells at three hours, to capture invasive cell behavior, indicated that invasive cells did exhibit a relocalized MTOC (Figure 4.3, right).

To further characterize differences in behavior of contractile and invasive cells, we tracked the localization of phosphorylated Zap70 Y319 in invasive cells; MTOC relocalization indicated that the IS had repositioned to the base of the array and thus TCR engagement may be localized to the base of the array as well. Immunostaining for phosphorylated Zap70 Y319 in invasive cells demonstrated relocalization to the base of the array, while still retaining punctate form (Figure 4.4 A). In keeping with the interest of resolving cellular activation components and cytoskeletal components, the localization profile of both F-actin and Myosin IIA were evaluated in invasive cells. F-actin demonstrated enrichment along the cell periphery, showing the greatest level of enrichment at the sites of cell contact with the sidewalls of micropillars. Myosin IIA did not show any preferential localization, though was noted to be present throughout the cell and not just enriched at the interface like with contractile cells. We next looked into the motivation for the invasive behavior. Both biochemical and mechanical properties are potential factors in driving cellular behavior, and the two would need to be deconstructed to resolve which was responsible for cellular invasion.

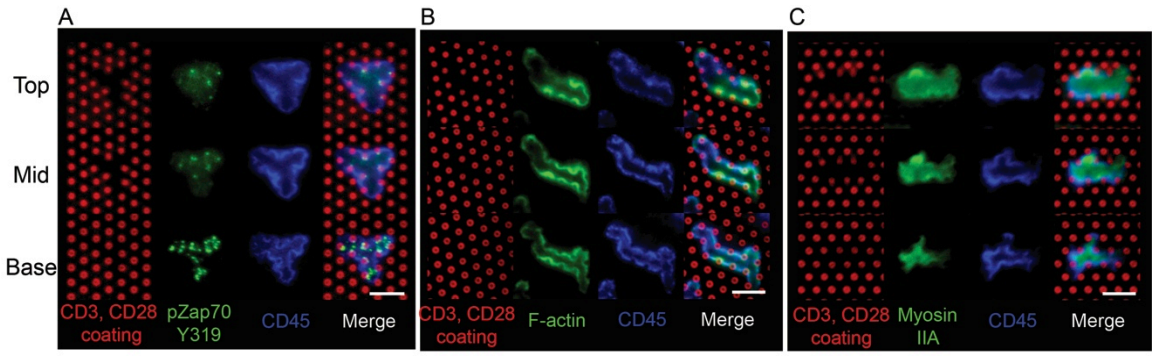

Figure 4.4. Protein redistribution in invasive cells. (A) Staining for TCR activation, indicated by phosphorylated Zap70 Y319, shows a relocalization of activating signal to the base of the array. (B) Staining for F-actin cytoskeleton showed distribution along the cell periphery, with substantial enrichment at the points of contact with micropillars. (C) Non-muscle Myosin IIA remains relatively diffuse throughout cells, though is physically segregated from the site of F-actin and CD45 enrichment along the perimeter.

Cell activation drives morphology

T cells that migrated to the base of the array exhibited a large degree of stability, which was impressive given the force exertion required to maintain displacement of the micropillars. Similar behavior has been observed in T cells as a function of their role as migratory cells. As previously described, T cells routinely penetrate through cell layers for a number of tasks, such as entering HEVs in the lymph node for activation by dendritic cells and passing through vascular endothelial layers to monitor peripheral tissues [115-118]. However, with the possible exception of HEV entry, these circumstances do not demonstrate transmigration in the presence of TCR activation.

Rather, an intricate multi-step pathway initially triggered by integrins, such as LFA-1 and VLA-4, and chemotactic cytokines that drive lymphocyte transmigration. To resolve

whether the observed invasive behavior of T cells was a result of topology or TCR activation, we looked for a way to isolate the TCR signal from the topology. Past literature, as well as work earlier in this thesis, point to soft lithography as a valid mechanism of selectively distributing protein. However, the high aspect ratio of the micropillar array made attempts to transfer of protein to the top of the pillars unreliable, as these features readily collapse under pressure. To this effect, we designed trenches, which would provide the topology necessary to enable cellular migration but with sufficient bulk to withstand the process of physically transferring protein.

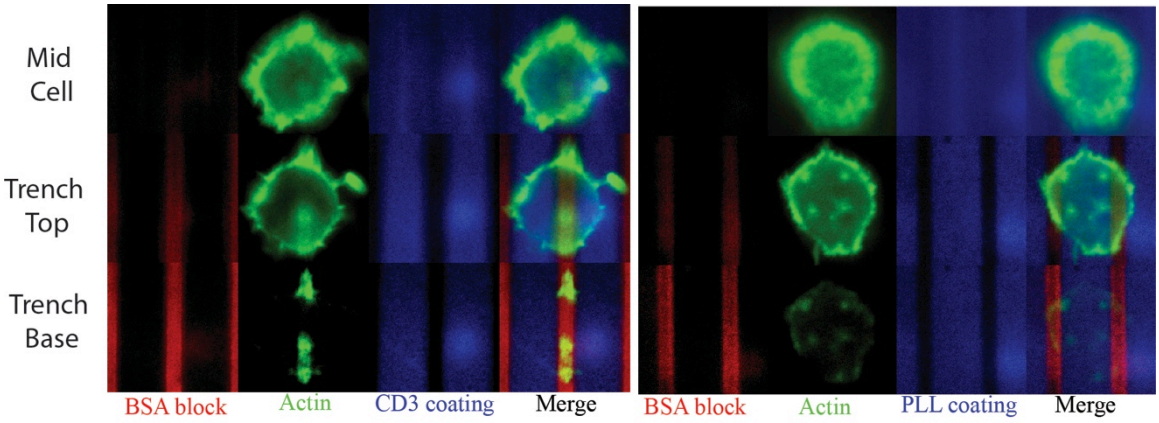

Figure 4.5. TCR activation induces morphological changes. T cells were activated on cellular trenches, where the planar top regions were coated via microcontact printing with either CD3 (left image, blue) or poly-L-lysine (PLL, right image, blue). The base and sides of the trenches were then backfilled with BSA (red) to ensure that any behavior pertaining to the trenches would be motivated by topology rather than protein interactions. Cells that were activated with CD3 ±CD28 extended filopedial protrusions into these trenches, as indicated by an actin stain (green). However, cells that were coated on PLL did not exhibit similar protrusions.

We applied selectively coated trenches to explore the driving force for T cell invasion into pillar arrays. To this effect, we compared the effects of transferring either activating

signal, targeting TCR ± CD28, or non-activating, poly-L-lysine [PLL], to the top of the surface, leaving the sides and bottom of the trench free of any coating. These regions were subsequently blocked with 5% BSA. Cells were seeded on these surfaces, where adhesion may occur at the top of the surface, and observed for morphological changes. T cells initially aligned with the direction of the trenches on both activating and non-activating surfaces, indicative of a preference to maximize contact area. Fixing and immunostaining cells at three hours, a timepoint chosen for the mixed behavior of T cells on micropillars, revealed that T cells on activating surfaces were capable of extending filopedia-like protrusions into these trench regions when triggered by TCR activation (Figure 4.5). These filopedia, like those in cells penetrating micropillars, were rich in F-actin. However, cells that were seeded on PLL did not generate these protrusions or show any effort to interact with the trenches.

These results collectively suggest that the transmigratory-like behavior noted on micropillars was in part driven by activating signal and also in part by surface topology. The introduction of the filopedial protrusions were a direct consequence of cellular activation. Likewise, the topology provided by both the micropillars and trenches enabled cellular migration in a manner that would be difficult to capture on a planar surface. Collectively, these works suggest that the characterization of a dynamically stable IS may be an artifact of work performed on lipid bilayers, where the bilayer offers a planar surface and puts up little resistance to remodeling by the T cell.

T cells experience forces during activation

T cell invasion into micropillars was an unanticipated outcome of TCR triggering. Moreover, the use of trenches demonstrated that actin-rich filopedial protrusions were triggered by activation. We next looked to put these results in context; earlier in this chapter, micropillars were applied to measure the forces exerted by T cells on their environment. Here we assess the mechanical properties and behavior of dendritic cells to gauge the forces exerted by an APC during IS dynamics.

Bone marrow-derived dendritic cells [bmDC] were cultured with granulocyte macrophage colony-stimulating factor [GM-CSF]: a standard process for deriving mature bmDCs. Mature bmDCs were then briefly characterized on planar fibronectin-coated surfaces and were subsequently evaluated for contractile forces in a process similar to what was used for measuring T cell forces (Figure 4.6 A,B). BmDC behavior was notably different than CD4 T cells; rather than exhibiting numerous phases, bmDCs went through an initial spreading phase, leading to a burst of force along the perimeter, and subsequently showed the greatest displacement along the perimeter of the cell. Like T cells, bmDCs forces, rather than displacements, were conserved across pillars of varying stiffness (Figure 4.6 C). The forces generated by bmDCs, however, were substantially larger than T cells, averaging 11.5 nN per cell, or 320 pn/μm^2. The results here are more tenuous, as they are measured when bmDCs are engaged by integrins, rather than by an interaction that is intended to directly simulate a T cell interaction. Unlike T cell receptor engagements, which have been successfully simulated with activating monoclonal antibodies, there has been less motivation to replicate the interaction from the APC side.

Future work may look to see if these noted forces are retained during T cell engagement.

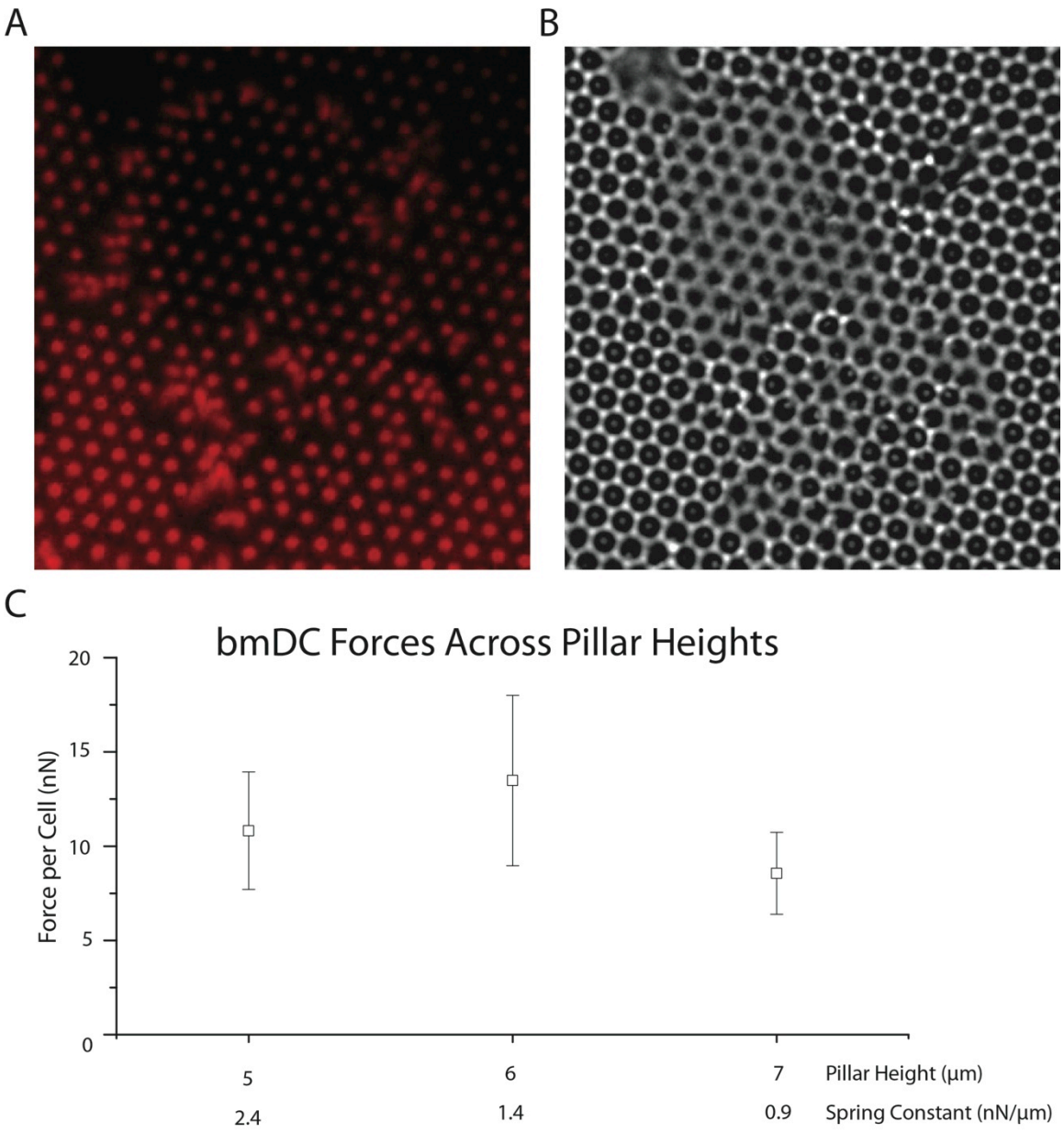

Figure 4.6. Measurement of bmDC forces (A) A representative image of a bmDC generating forces on 5 μm pillars, along with (B) the accompanying brightfield image. (C) Measurement of bmDC forces across pillars of different spring constants demonstrated a behavior similar to T cells, where force generation rather than pillar displacement was consistent.

4.5 Discussion

Studies that look at T cell activation using planar glass substrates have been integral in the identification of key proteins that are relocalized during IS maturation; moreover, these studies have validated that T cell activation may proceed using artificial APCs. The subsequent application of lipid bilayers and the temporal resolution of protein migration through photoconjugated fluorescent tags have together led to insights into the spatial-temporal dynamics of T cell activation: pinnacled by the bull's eye alignment of activation factors. In this chapter, we expand on previous works by using 3-D topology to characterize cell behavior, both with respect to cell migration and protein localization over time. After an initial phase, lasting roughly one hour, of exerting contractile forces on micropillars, T cells begin to extend filopedial projections to identify the topology of their environment. These protrusions were precursors for the relocalization of the cell to the base of the array. Using fabricated microtrenches, we identify that while these protrusions are initiated by TCR activation, cellular relocalization is driven by TCR engagement. The overall behavior of transmigration appears to deter cellular activation, leading to a delay in MTOC localization to the activating surface as well as decreased production of IL-2 relative to a planar surface.

There is some overlap between these findings and those previously described by *Husson et al*, where a single protrusion from the cell is observed exerting forces on a TCR-activating bead [31]. Here however, we demonstrate that these protrusions are initiated by TCR activation but do not extend exclusively towards the site of TCR engagement. Mapping of bmDC forces demonstrate that T cell plasticity is not without purpose.

BmDCs, and likely other APCs, demonstrate the ability to exert substantially greater forces than T cells, suggesting that the freely diffusing lipid bilayers that are used to track IS dynamics may be further improved with the introduction of resistance.

Chapter 5 – Conclusion

5.1 Summary

This body of work applies a range of techniques that collectively are used to investigate the subcellular processes that drive CD4+ T cell activation. The primary focus is a subcellular study of CD28-driven costimulation, where both the initial pathway enabling its coupling with TCR signaling as well as a number of its downstream endpoints are described. Coupling of the TCR and CD28 pathways is mediated by the Src kinase Lck, which is regulated by its protein interactions and the cytoskeletal network. The regulation of Lck diffusion in human T cells confers spatial sensitivity to the relative positions of TCR and CD28. The sensitivity observed in human cells is not shared in mouse cells that are sourced and purified in a comparable manner, and Lck plays a less significant role in conferring spatial sensitivity to the relative positions of TCR and CD28 in mouse T cells. Rather, previous work points to the relative distribution of CD28 across the interface, independent of TCR distribution, as the driving force in augmenting cellular activation in mouse cells [24]. The significance of this finding has not been resolved in vivo, but we postulate that this sensitivity imports significance during the formation of the immune synapse, where microclusters of TCR and CD28 comigrate to the central region of the synapse and later segregate within this central region. Modulation of spatial control through the cytoskeleton may either play a role in restricting TCR-CD28 communication when coclustered or may also be a mechanism to enable communication with the local depletion of actin from the central synapse. Cytoskeletal depletion in the context of this latter concept would share a similar, though not necessarily redundant, role as CD45

displacement towards the peripheral of the synapse.

The work in this thesis also highlights the role of the TCR in enabling contractile forces, as measured on micropillar arrays. Costimulation through CD28 is found to augment this process; introduction of this costimulatory interaction increases contractile forces by a substantial level. Force measurements via micropillar arrays is also used to identify the role of CD28 as a mechanoreceptor. Triggering of CD28 enhances contractile forces through a process that is not dependent on its manner of presentation, highlighting its role as a mechanoresponsive but not mechanosensitive receptor. Given the complexity of the CD28 pathway, there are numerous routes through which this mechanoresponse may be mediated. We highlight that this augmentation is dependent on the role of PI3 kinase and its interaction with the cytoplasmic pathway. Moreover, PDK1, downstream of PI3 kinase, is responsible for forces generated through both the TCR and CD28 pathway. This is a substantial first step in the mapping of this newly classified mechanoresponsive receptor.

Work assessing the process of T cell activation on micropillar arrays also demonstrated the intricacy of the activation process; the ability to interact with an artificial substrate of complex topology revealed a new facet to T cell behavior. Whereas studies that activate of T cells on planar surfaces show the T cell to be relatively immobile during activation, micropillars introduce a new direction of cellular migration, into the array, which cells actively pursue in spite of the increased forces needed to pursue this direction of motion. Spatially segregating the topology from the activating signal, through cellular trenches,

demonstrates that TCR triggering is sufficient to initiate the extension of filopedia-like protrusions that T cells use to explore the topology of their environment.

5.2 Future Directions

Force-measuring bilayers

While the micropatterning techniques applied provide the aforementioned insights into spatial dynamics, new studies are needed to resolve the temporal relevance of induced activation. The immobilization of proteins provided by micropatterned surfaces currently offers a compliment to work with lipid bilayers, where T cells may drive the localization of proteins within the synapse with little resistance. Micropillar arrays were used to quantify the forces generated during cellular activation, which were shown to be substantial. This approach of analysis using two dichotomized systems has its uses, but ultimately comes with the caveat of never fully capturing a truly representative environment. Future work in this direction may seek to find a compromise between the two: where there is greater resistance to protein relocalization than what lipid bilayers currently permit. Past work on corralled bilayers has shown success in deterring the rate of membrane diffusion. Though nonlinear in relationship, controlling the gap size and spacing of corrals would be a functional method of regulating lateral diffusion, a process that can be overcome through increased force exertion. Application of corralled bilayers to the study of immune synapse formation may lead to new insights into the mechanics of TCR and CD28 integration, and the role of increased contractile forces induced by CD28 to this process. Corralled bilayers permit the fluidity of membrane reorganization without

the compromise of free mobility; rather modulating the gap size and spacing enables the control of resistance to lateral flow.

Cytoskeletal redistribution in lieu of depletion

Also in the direction of spatial sensitivity to TCR and CD28 integration, the actin cytoskeleton was demonstrated to be largely responsible for the deterred diffusion of Lck in human T cells. The spatial correlation of Lck and F-actin in LatB treated cells also implicated that Lck diffusion is actively regulated. However, immunostaining for the cytoskeleton of cells invading micropillars revealed substantial F-actin enrichment along the periphery, in contact with the micropillars, whereas TCR triggering was localized to the base of the array. This demonstrates an alternative approach, other than LatB-induced inhibition of F-actin assembly, where the dense cytoskeleton is relocalized from the IS rather than deconstructed throughout the cell. We postulate here that relocalization of the cytoskeleton through similar techniques will desensitize human T cells to segregation of TCR-CD28 triggering. IL-2 secretion was measured, and demonstrated lower levels of secretion in invasive cells than those on planar PDMS; however, invasive cells on micropillars form smaller synapses than those on planar surfaces. Previous work has demonstrated that the breadth of the IS plays a significant role in IL-2 secretion.

Vetting preclinical models

There is also a need to further resolve and expand upon observed differences in human and mouse cells, where both the diffusion of Lck and the extent of F-actin enrichment at the interface differ. Work in this direction may be multifaceted but ultimately will be

driven by practical significance, which is to develop more precise models in the context of clinical endpoints. Early work has showed that the response to rigidity is fundamentally different in activating mouse and human T cells. Whereas human T cells show increasing levels of IL-2 production on softer surfaces, mouse T cells demonstrated increasing levels of IL-2 production on stiffer surfaces. However these experiments were not initially performed with the intention of a direct comparison. Both the methods and range of surface stiffness tested differ slightly, encouraging a more direct approach in comparing the responses. It would also be incumbent to propose a mechanism for this underlying difference. The cytoskeletal network, which was noted to exhibit fundamental differences in the two species, makes for a compelling candidate.

A role for rigidity becomes significant in preclinical studies, where the properties of cells cultured on plastics may vary substantially from those that are derived in vivo.

Pathways to costimulation

The family of T cell costimulatory factors is categorized by protein receptors that interact with B7 proteins on the APC to augment T cell activation. Two B7 proteins, B7.1 & B7.2, were identified nearly twenty years ago: predating cluster differentiation [CD] nomenclature [119, 120]. Though these two proteins, now respectively named CD80 and CD86, have been well-characterized, the few differences that have been found do not drastically dichotomize the two [121-125]. Though current research indicates that the APC-side of costimulation exhibits nuanced differences, the T cell-side of the interaction has greater diversity in receptors that collectively manifest a multifarious response that

relies on expression levels and kinetics. The work in this thesis focuses exclusively on the CD28 pathway and its involvement in augmenting TCR activation. However, CD28 is not the exclusive costimulatory receptor; rather it is the most studied receptor. The family of T cell costimulatory receptors also includes cytotoxic T lymphocyte antigen 4 [CTLA-4], inducible costimulatory molecule [ICOS], BTLA and PD-1. Along with CD28, ICOS acts as a positive costimulatory factor.

The remaining three receptors, CTLA-4, BTLA and PD-1, play a role in negative modulation cellular activation: effectively terminating cellular activation, which inhibits T cell proliferation and leads to apoptosis [126]. Of the three, CTLA-4 was the first to be identified and is currently the most extensively studied. Recent work by Yokosuka et al. looks at the kinetics of CD28 and CTLA-4 competition for B7 interaction, demonstrating real-time competition between the two ligands that result in changes in spatial localization within the IS [127]. Here, CTLA-4 overexpression was found to block localization of CD28-PKCθ microclusters to the central IS: effectively abrogating positive costimulation through CD28. While it has been known for some time that CTLA-4 has a higher affinity for B7 ligands than CD28, this insight into a mechanism that manifests through spatial replacement of CD28 for CTLA-4 motivates exploration into the spatial regulation of CTLA-4 negative stimulation. The aims in this thesis, identification of a mechanism for spatial regulation of CD28-induced costimulation and an exploration into the role of mechanotransduction in costimulation, provide a framework for deconstructing the process of negative costimulation. Other than their intended endpoint for T cell differentiation, another fundamental difference between the

two receptors is their localization in resting naïve T cells. Whereas CD28 is constitutively expressed on the cell membrane, CTLA-4 is retained internally and is transported to the surface as T cell activation initiates.

5.3 Significance

Over the past few decades, the field of immunology has matured along with our understanding of the mechanisms that modulate the immune system. The dual roles of responding to foreign antigens and self-tolerating native tissues is a daunting task. Helper T cells play a distinct and critical role in immunesurveillance, as is evident in situations where their function or numbers are compromised such as with HIV. The work in this thesis introduces new metrics to assess T cell activation, which may be used to better characterize the impact of compromised CD4 T cells. Future work may look to reintroduce HIV-resistant CD4 T cells through the application of CARs that pervade CTLA-4 assisted viral infection.

One of the underlying concepts of this thesis is subcellular organization: both in regards to its construction and its manifestation. That cells construct complex domains is well characterized in many systems [52, 53]. Here we focus on the IS junction between a mature APC and a naïve T cell to demonstrate a mechanism for pathway convergence that is driven by spatiotemporal dynamics. The work in this thesis develops a model where the convergence of two pathways can be spatially regulated by the diffusivity and regulation of an intermediate. Development of such models affords opportunities to study the synergism between receptor pairs in other cellular contexts.

Though indications of disparities have existed for some time, it is becoming increasingly clear that what we consider to be our most robust preclinical models harbor nuanced differences that may ultimately misdirect our clinical endeavors. The rising cost of new drug approval has been marginally impacted by updated guidelines by the FDA that aim to minimize adverse effects. Rather, one of the greatest sources of high drug costs is late-stage failures. The cost of taking a typical drug from identified substance to NDA approval has an average cost of $300 million. However, adjusting this price tag with the cost of failed INDs raises the average cost to $1 billion per drug. Advances that map the shortcomings of our preclinical models would do much to help reduce these costs. Efforts to further humanize mouse models, much in the same way that mouse-derived monoclonal antibodies have been humanized to reduce the immunogenicity of antibody-based therapies. Already, extensive research has gone towards the development of these humanized mouse models for specific disease categories [128-130]. Future work in this direction will look to bridge newly discovered disparities.

References

1. Roger, V.L., et al., *Heart disease and stroke statistics--2012 update: a report from the American Heart Association.* Circulation, 2012. **125**(1): p. e2-e220.

2. Schottenfeld, D., et al., *Current perspective on the global and United States cancer burden attributable to lifestyle and environmental risk factors.* Annu Rev Public Health, 2013. **34**: p. 97-117.

3. Hanahan, D. and R.A. Weinberg, *The hallmarks of cancer.* Cell, 2000. **100**(1): p. 57-70.

4. Hanahan, D. and R.A. Weinberg, *Hallmarks of cancer: the next generation.* Cell, 2011. **144**(5): p. 646-74.

5. Spyridonidis, A. and M. Liga, *A long road of T-cells to cure cancer: from adoptive immunotherapy with unspecific cellular products to donor lymphocyte infusions and transfer of engineered tumor-specific T-cells.* Am J Blood Res, 2012. **2**(2): p. 98-104.

6. Palucka, K. and J. Banchereau, *Cancer immunotherapy via dendritic cells.* Nat Rev Cancer, 2012. **12**(4): p. 265-77.

7. Schott, M., *Immunesurveillance by dendritic cells: potential implication for immunotherapy of endocrine cancers.* Endocr Relat Cancer, 2006. **13**(3): p. 779-95.

8. Schott, M. and J. Seissler, *Dendritic cell vaccination: new hope for the treatment of metastasized endocrine malignancies.* Trends Endocrinol Metab, 2003. **14**(4): p. 156-62.

9. Tacken, P.J., et al., *Dendritic-cell immunotherapy: from ex vivo loading to in vivo targeting.* Nat Rev Immunol, 2007. **7**(10): p. 790-802.

10. White, D.M., et al., *Rapid immune responses to a botulinum neurotoxin Hc subunit vaccine through in vivo targeting to antigen-presenting cells.* Infect Immun, 2011. **79**(8): p. 3388-96.

11. Mosmann, T.R., et al., *Two types of murine helper T cell clone. I. Definition according to profiles of lymphokine activities and secreted proteins.* J Immunol, 1986. **136**(7): p. 2348-57.

12. Mosmann, T.R. and R.L. Coffman, *TH1 and TH2 cells: different patterns of lymphokine secretion lead to different functional properties.* Annu Rev Immunol, 1989. **7**: p. 145-73.

13. Homey, B., *[After TH1/TH2 now comes Treg/TH17: significance of T helper cells in immune response organization]*. Hautarzt, 2006. **57**(8): p. 730-2.

14. Forsthuber, T.G. and N. Ji, *Quo vadis Th1 and Th2 cells in autoimmunity and infectious diseases: Th17 cells, the new kid on the block.* Expert Rev Clin Immunol, 2007. **3**(3): p. 251-4.

15. Klebanoff, C.A., L. Gattinoni, and N.P. Restifo, *Sorting through subsets: which T-cell populations mediate highly effective adoptive immunotherapy?* J Immunother, 2012. **35**(9): p. 651-60.

16. O'Shea, J.J. and W.E. Paul, *Mechanisms underlying lineage commitment and plasticity of helper CD4+ T cells.* Science, 2010. **327**(5969): p. 1098-102.

17. Kim, J.M., J.P. Rasmussen, and A.Y. Rudensky, *Regulatory T cells prevent catastrophic autoimmunity throughout the lifespan of mice.* Nat Immunol, 2007. **8**(2): p. 191-7.

18. Tseng, S.Y., et al., *T cell-dendritic cell immunological synapses contain TCR-dependent CD28-CD80 clusters that recruit protein kinase C theta.* J Immunol, 2008. **181**(7): p. 4852-63.

19. Yokosuka, T., et al., *Spatiotemporal regulation of T cell costimulation by TCR-CD28 microclusters and protein kinase C theta translocation.* Immunity, 2008. **29**(4): p. 589-601.

20. Grakoui, A., et al., *The immunological synapse: a molecular machine controlling T cell activation.* Science, 1999. **285**(5425): p. 221-7.

21. Yokosuka, T., et al., *Newly generated T cell receptor microclusters initiate and sustain T cell activation by recruitment of Zap70 and SLP-76.* Nat Immunol, 2005. **6**(12): p. 1253-62.

22. Yokosuka, T. and T. Saito, *The immunological synapse, TCR microclusters, and T cell activation.* Curr Top Microbiol Immunol, 2010. **340**: p. 81-107.

23. Yokosuka, T. and T. Saito, *Dynamic regulation of T-cell costimulation through TCR-CD28 microclusters.* Immunol Rev, 2009. **229**(1): p. 27-40.

24. Shen, K., et al., *Micropatterning of costimulatory ligands enhances CD4+ T cell function.* Proc Natl Acad Sci U S A, 2008. **105**(22): p. 7791-6.

25. Doh, J. and D.J. Irvine, *Immunological synapse arrays: patterned protein surfaces that modulate immunological synapse structure formation in T cells.* Proc Natl Acad Sci U S A, 2006. **103**(15): p. 5700-5.

26. Mossman, K.D., et al., *Altered TCR signaling from geometrically repatterned immunological synapses.* Science, 2005. **310**(5751): p. 1191-3.

27. Yu, C.H., et al., *Altered actin centripetal retrograde flow in physically restricted immunological synapses.* PLoS One, 2010. **5**(7): p. e11878.

28. Bunnell, S.C., et al., *Dynamic actin polymerization drives T cell receptor-induced spreading: a role for the signal transduction adaptor LAT.* Immunity, 2001. **14**(3): p. 315-29.

29. Kaizuka, Y., et al., *Mechanisms for segregating T cell receptor and adhesion molecules during immunological synapse formation in Jurkat T cells.* Proc Natl Acad Sci U S A, 2007. **104**(51): p. 20296-301.

30. Hsu, C.J. and T. Baumgart, *Spatial association of signaling proteins and F-actin effects on cluster assembly analyzed via photoactivation localization microscopy in T cells.* PLoS One, 2011. **6**(8): p. e23586.

31. Husson, J., et al., *Force generation upon T cell receptor engagement.* PLoS One, 2011. **6**(5): p. e19680.

32. Ueda, H., et al., *CD4+ T-cell synapses involve multiple distinct stages.* Proc Natl Acad Sci U S A, 2011. **108**(41): p. 17099-104.

33. Deeks, S.G., et al., *A phase II randomized study of HIV-specific T-cell gene therapy in subjects with undetectable plasma viremia on combination antiretroviral therapy.* Mol Ther, 2002. **5**(6): p. 788-97.

34. van Lunzen, J., et al., *Investigations on autologous T-cells for adoptive immunotherapy of AIDS.* Adv Exp Med Biol, 1995. **374**: p. 57-70.

35. Riddell, S.R. and P.D. Greenberg, *Cellular adoptive immunotherapy after bone marrow transplantation.* Cancer Treat Res, 1995. **76**: p. 337-69.

36. Basse, P.H., *Tissue distribution and tumor localization of effector cells in adoptive immunotherapy of cancer.* APMIS Suppl, 1995. **55**: p. 1-28.

37. Gaundar, S.S., et al., *In vitro generation of influenza-specific polyfunctional CD4+ T cells suitable for adoptive immunotherapy.* Cytotherapy, 2012. **14**(2): p. 182-93.

38. Al-Khami, A.A., S. Mehrotra, and M.I. Nishimura, *Adoptive immunotherapy of cancer: Gene transfer of T cell specificity.* Self Nonself, 2011. **2**(2): p. 80-84.

39. August, A. and B. Dupont, *CD28 of T lymphocytes associates with phosphatidylinositol 3-kinase.* Int Immunol, 1994. **6**(5): p. 769-74.

40. Alegre, M.L., K.A. Frauwirth, and C.B. Thompson, *T-cell regulation by CD28 and CTLA-4.* Nat Rev Immunol, 2001. **1**(3): p. 220-8.

41. Kaga, S., et al., *Stimulation of CD28 with B7-2 promotes focal adhesion-like cell contacts where Rho family small G proteins accumulate in T cells.* J Immunol, 1998. **160**(1): p. 24-7.

42. King, P.D., et al., *Analysis of CD28 cytoplasmic tail tyrosine residues as regulators and substrates for the protein tyrosine kinases, EMT and LCK.* J Immunol, 1997. **158**(2): p. 580-90.

43. Raab, M., et al., *p56Lck and p59Fyn regulate CD28 binding to phosphatidylinositol 3-kinase, growth factor receptor-bound protein GRB-2, and T cell-specific protein-tyrosine kinase ITK: implications for T-cell costimulation.* Proc Natl Acad Sci U S A, 1995. **92**(19): p. 8891-5.

44. King, C.L., et al., *CD28 activation promotes Th2 subset differentiation by human CD4+ cells.* Eur J Immunol, 1995. **25**(2): p. 587-95.

45. Ferguson, S.E., et al., *CD28 is required for germinal center formation.* J Immunol, 1996. **156**(12): p. 4576-81.

46. Freeman, G.J., et al., *Cloning of B7-2: a CTLA-4 counter-receptor that costimulates human T cell proliferation.* Science, 1993. **262**(5135): p. 909-11.

47. Brown, G.C. and B.N. Kholodenko, *Spatial gradients of cellular phospho-proteins.* FEBS Lett, 1999. **457**(3): p. 452-4.

48. Neves, S.R., et al., *Cell shape and negative links in regulatory motifs together control spatial information flow in signaling networks.* Cell, 2008. **133**(4): p. 666-80.

49. Neves, S.R. and R. Iyengar, *Models of spatially restricted biochemical reaction systems.* J Biol Chem, 2009. **284**(9): p. 5445-9.

50. Dustin, M.L., et al., *T cell-dendritic cell immunological synapses.* Curr Opin Immunol, 2006. **18**(4): p. 512-6.

51. Saggioro, D., et al., *Mechanism of action of the monosialoganglioside GM1 as a modulator of CD4 expression. Evidence that GM1-CD4 interaction triggers dissociation of p56lck from CD4, and CD4 internalization and degradation.* J Biol Chem, 1993. **268**(2): p. 1368-75.

52. Desai, R.A., et al., *Subcellular spatial segregation of integrin subtypes by patterned multicomponent surfaces.* Integr Biol (Camb), 2011. **3**(5): p. 560-7.

53. Shi, P., K. Shen, and L.C. Kam, *Local presentation of L1 and N-cadherin in multicomponent, microscale patterns differentially direct neuron function in vitro.* Dev Neurobiol, 2007. **67**(13): p. 1765-76.

54. Hudrisier, D., et al., *Capture of target cell membrane components via trogocytosis is triggered by a selected set of surface molecules on T or B cells.* J Immunol, 2007. **178**(6): p. 3637-47.

55. Katsch, K., et al., *Actin-dependent activation of serum response factor in T cells by the viral oncoprotein tip.* Cell Commun Signal, 2012. **10**(1): p. 5.

56. Nolz, J.C., et al., *The WAVE2 complex regulates T cell receptor signaling to integrins via Abl- and CrkL-C3G-mediated activation of Rap1.* J Cell Biol, 2008. **182**(6): p. 1231-44.

57. Fraser, J.D., et al., *Regulation of interleukin-2 gene enhancer activity by the T cell accessory molecule CD28.* Science, 1991. **251**(4991): p. 313-6.

58. Street, N.E., et al., *Heterogeneity of mouse helper T cells. Evidence from bulk cultures and limiting dilution cloning for precursors of Th1 and Th2 cells.* J Immunol, 1990. **144**(5): p. 1629-39.

59. Jonsson, P., et al., *A method improving the accuracy of fluorescence recovery after photobleaching analysis.* Biophys J, 2008. **95**(11): p. 5334-48.

60. Prasad, K.V., et al., *Regulation of CD4-p56lck-associated phosphatidylinositol 3-kinase (PI 3-kinase) and phosphatidylinositol 4-kinase (PI 4-kinase).* Philos Trans R Soc Lond B Biol Sci, 1993. **342**(1299): p. 35-42.

61. Holdorf, A.D., et al., *Regulation of Lck activity by CD4 and CD28 in the immunological synapse.* Nat Immunol, 2002. **3**(3): p. 259-64.

62. Delon, J., et al., *Imaging antigen recognition by naive CD4+ T cells: compulsory cytoskeletal alterations for the triggering of an intracellular calcium response.* Eur J Immunol, 1998. **28**(2): p. 716-29.

63. Tee, S.Y., A.R. Bausch, and P.A. Janmey, *The mechanical cell.* Curr Biol, 2009. **19**(17): p. R745-8.

64. Ike, H., et al., *Mechanism of Lck recruitment to the T-cell receptor cluster as studied by single-molecule-fluorescence video imaging.* Chemphyschem, 2003. **4**(6): p. 620-6.

65. Billadeau, D.D., J.C. Nolz, and T.S. Gomez, *Regulation of T-cell activation by the cytoskeleton.* Nat Rev Immunol, 2007. **7**(2): p. 131-43.

66. Cane, S., S. Ponnappan, and U. Ponnappan, *Impairment of non-muscle myosin IIA in human CD4+ T cells contributes to functional deficits in the elderly.* Cell Mol Immunol, 2012. **9**(1): p. 86-96.

67. Chichili, G.R., A.D. Westmuckett, and W. Rodgers, *T cell signal regulation by the actin cytoskeleton.* J Biol Chem, 2010. **285**(19): p. 14737-46.

68. Annunziato, F. and S. Romagnani, *Do studies in humans better depict Th17 cells?* Blood, 2009. **114**(11): p. 2213-9.

69. McGovern, J.L., et al., *Th17 cells are restrained by Treg cells via the inhibition of interleukin-6 in patients with rheumatoid arthritis responding to anti-tumor necrosis factor antibody therapy.* Arthritis Rheum, 2012. **64**(10): p. 3129-38.

70. Ju, J.H., et al., *Modulation of STAT-3 in rheumatoid synovial T cells suppresses Th17 differentiation and increases the proportion of Treg cells.* Arthritis Rheum, 2012. **64**(11): p. 3543-52.

71. Judokusumo, E., et al., *Mechanosensing in T lymphocyte activation.* Biophys J, 2012. **102**(2): p. L5-7.

72. O'Connor, R.S., et al., *Substrate rigidity regulates human T cell activation and proliferation.* J Immunol, 2012. **189**(3): p. 1330-9.

73. Chan, A.C., et al., *Differential expression of ZAP-70 and Syk protein tyrosine kinases, and the role of this family of protein tyrosine kinases in TCR signaling.* J Immunol, 1994. **152**(10): p. 4758-66.

74. Rivas, F.V., et al., *Actin cytoskeleton regulates calcium dynamics and NFAT nuclear duration.* Mol Cell Biol, 2004. **24**(4): p. 1628-39.

75. Krummel, M., et al., *Thirty-six views of T-cell recognition.* Philos Trans R Soc Lond B Biol Sci, 2000. **355**(1400): p. 1071-6.

76. Tan, J.L., et al., *Cells lying on a bed of microneedles: an approach to isolate mechanical force.* Proc Natl Acad Sci U S A, 2003. **100**(4): p. 1484-9.

77. Ghassemi, S., et al., *Cells test substrate rigidity by local contractions on submicrometer pillars.* Proc Natl Acad Sci U S A, 2012. **109**(14): p. 5328-33.

78. Yang, M.T., et al., *Assaying stem cell mechanobiology on microfabricated elastomeric substrates with geometrically modulated rigidity.* Nat Protoc, 2011. **6**(2): p. 187-213.

79. Thevenaz, P., U.E. Ruttimann, and M. Unser, *A pyramid approach to subpixel registration based on intensity.* IEEE Trans Image Process, 1998. **7**(1): p. 27-41.

80. Sbalzarini, I.F. and P. Koumoutsakos, *Feature point tracking and trajectory analysis for video imaging in cell biology.* J Struct Biol, 2005. **151**(2): p. 182-95.

81. Saez, A., et al., *Is the mechanical activity of epithelial cells controlled by deformations or forces?* Biophys J, 2005. **89**(6): p. L52-4.

82. Vicente-Manzanares, M., et al., *Non-muscle myosin II takes centre stage in cell adhesion and migration.* Nat Rev Mol Cell Biol, 2009. **10**(11): p. 778-90.

83. Rossy, J., D.J. Williamson, and K. Gaus, *How does the kinase Lck phosphorylate the T cell receptor? Spatial organization as a regulatory mechanism.* Front Immunol, 2012. **3**: p. 167.

84. Gaus, K., et al., *Condensation of the plasma membrane at the site of T lymphocyte activation.* J Cell Biol, 2005. **171**(1): p. 121-31.

85. Riha, P. and C.E. Rudd, *CD28 co-signaling in the adaptive immune response.* Self Nonself, 2010. **1**(3): p. 231-240.

86. Pages, F., et al., *Two distinct intracytoplasmic regions of the T-cell adhesion molecule CD28 participate in phosphatidylinositol 3-kinase association.* Journal of Biological Chemistry, 1996. **271**(16): p. 9403-9409.

87. Sanchez-Lockhart, M., et al., *Cutting edge: CD28-mediated transcriptional and posttranscriptional regulation of IL-2 expression are controlled through different signaling pathways.* J Immunol, 2004. **173**(12): p. 7120-4.

88. Boomer, J.S. and J.M. Green, *An enigmatic tail of CD28 signaling.* Cold Spring Harb Perspect Biol, 2010. **2**(8): p. a002436.

89. Dodson, L.F., et al., *Targeted knock-in mice expressing mutations of CD28 reveal an essential pathway for costimulation.* Mol Cell Biol, 2009. **29**(13): p. 3710-21.

90. Bitting, R.L. and A.J. Armstrong, *Targeting the PI3K/Akt/mTOR pathway in castration-resistant prostate cancer.* Endocr Relat Cancer, 2013.

91. Knight, Z.A., *For a PDK1 inhibitor, the substrate matters.* Biochem J, 2011. **433**(2): p. e1-2.

92. Najafov, A., et al., *Characterization of GSK2334470, a novel and highly specific inhibitor of PDK1.* Biochem J, 2011. **433**(2): p. 357-69.

93. Najafov, A., N. Shpiro, and D.R. Alessi, *Akt is efficiently activated by PIF-pocket- and PtdIns(3,4,5)P3-dependent mechanisms leading to resistance to PDK1 inhibitors.* Biochem J, 2012. **448**(2): p. 285-95.

94. Raimondi, C., et al., *A novel regulatory mechanism links PLCgamma1 to PDK1.* J Cell Sci, 2012. **125**(Pt 13): p. 3153-63.

95. Park, E.J., et al., *Distinct roles for LFA-1 affinity regulation during T-cell adhesion, diapedesis, and interstitial migration in lymph nodes.* Blood, 2010. **115**(8): p. 1572-81.

96. Azzali, G., et al., *The "intraendothelial canalicular formation": the route for lymphocyte diapedesis at the level of peripheral and mucosa-associated lymphoid tissue HEVs.* Acta Biomed, 2010. **81**(1): p. 5-20.

97. Tseng, S.Y., M. Liu, and M.L. Dustin, *CD80 cytoplasmic domain controls localization of CD28, CTLA-4, and protein kinase Ctheta in the immunological synapse.* J Immunol, 2005. **175**(12): p. 7829-36.

98. Brasel, K., et al., *Generation of murine dendritic cells from flt3-ligand-supplemented bone marrow cultures.* Blood, 2000. **96**(9): p. 3029-39.

99. Maroof, A., *Generation of murine bone-marrow-derived dendritic cells.* Methods Mol Med, 2001. **64**: p. 191-8.

100. Finetti, F., et al., *Intraflagellar transport: a new player at the immune synapse.* Trends Immunol, 2011. **32**(4): p. 139-45.

101. Wheatley, D.N., *Primary cilia in normal and pathological tissues.* Pathobiology, 1995. **63**(4): p. 222-38.

102. Kozminski, K.G., *Intraflagellar transport--the "new motility" 20 years later.* Mol Biol Cell, 2012. **23**(5): p. 751-3.

103. Jeurissen, S.H., et al., *Lymphocyte migration into the lamina propria of the gut is mediated by specialized HEV-like blood vessels.* Immunology, 1987. **62**(2): p. 273-7.

104. Faveeuw, C., G. Preece, and A. Ager, *Transendothelial migration of lymphocytes across high endothelial venules into lymph nodes is affected by metalloproteinases.* Blood, 2001. **98**(3): p. 688-95.

105. Bai, Z., et al., *Constitutive Lymphocyte Transmigration across the Basal Lamina of High Endothelial Venules Is Regulated by the Autotaxin/Lysophosphatidic Acid Axis.* J Immunol, 2013. **190**(5): p. 2036-48.

106. Gueant, J.L., et al., *Molecular and cellular effects of vitamin B12 in brain, myocardium and liver through its role as co-factor of methionine synthase.* Biochimie, 2013.

107. Truong, N.C., et al., *Postnatal rosiglitazone administration to neonatal rat pups does not alter the young adult metabolic phenotype.* Neonatology, 2012. **101**(3): p. 217-24.

108. Narayan, K., et al., *Intrathymic programming of effector fates in three molecularly distinct gammadelta T cell subtypes.* Nat Immunol, 2012. **13**(5): p. 511-8.

109. Caron, M.M., et al., *Activation of NF-kappaB/p65 facilitates early chondrogenic differentiation during endochondral ossification.* PLoS One, 2012. **7**(3): p. e33467.

110. Sojka, D.K. and D.J. Fowell, *Regulatory T cells inhibit acute IFN-gamma synthesis without blocking T-helper cell type 1 (Th1) differentiation via a compartmentalized requirement for IL-10.* Proc Natl Acad Sci U S A, 2011. **108**(45): p. 18336-41.

111. Chung, Y., et al., *Critical regulation of early Th17 cell differentiation by interleukin-1 signaling.* Immunity, 2009. **30**(4): p. 576-87.

112. Kupfer, A., S.L. Swain, and S.J. Singer, *The specific direct interaction of helper T cells and antigen-presenting B cells. II. Reorientation of the microtubule organizing center and reorganization of the membrane-associated cytoskeleton inside the bound helper T cells.* J Exp Med, 1987. **165**(6): p. 1565-80.

113. Gomez, J., et al., *Role of NF-kappaB in the control of apoptotic and proliferative responses in IL-2-responsive T cells.* Front Biosci, 1997. **2**: p. d49-60.

114. Arima, N., et al., *IL-2-induced growth of CD8+ T cell prolymphocytic leukemia cells mediated by NF-kappaB induction and IL-2 receptor alpha expression.* Leuk Res, 1998. **22**(3): p. 265-73.

115. Sandig, M., E. Negrou, and K.A. Rogers, *Changes in the distribution of LFA-1, catenins, and F-actin during transendothelial migration of monocytes in culture.* J Cell Sci, 1997. **110 (Pt 22)**: p. 2807-18.

116. Hourihan, H., T.D. Allen, and A. Ager, *Lymphocyte migration across high endothelium is associated with increases in alpha 4 beta 1 integrin (VLA-4) affinity.* J Cell Sci, 1993. **104 (Pt 4)**: p. 1049-59.

117. Ager, A. and S. Mistry, *Interaction between lymphocytes and cultured high endothelial cells: an in vitro model of lymphocyte migration across high endothelial venule endothelium.* Eur J Immunol, 1988. **18**(8): p. 1265-74.

118. Granger, D.N. and P. Kubes, *The microcirculation and inflammation: modulation of leukocyte-endothelial cell adhesion.* J Leukoc Biol, 1994. **55**(5): p. 662-75.

119. Caux, C., et al., *B70/B7-2 is identical to CD86 and is the major functional ligand for CD28 expressed on human dendritic cells.* J Exp Med, 1994. **180**(5): p. 1841-7.

120. Freeman, G.J., et al., *B7, a new member of the Ig superfamily with unique expression on activated and neoplastic B cells.* J Immunol, 1989. **143**(8): p. 2714-22.

121. Linsley, P.S., et al., *Human B7-1 (CD80) and B7-2 (CD86) bind with similar avidities but distinct kinetics to CD28 and CTLA-4 receptors.* Immunity, 1994. **1**(9): p. 793-801.

122. Melichar, B., et al., *Expression of costimulatory molecules CD80 and CD86 and their receptors CD28, CTLA-4 on malignant ascites CD3+ tumour-infiltrating lymphocytes (TIL) from patients with ovarian and other types of peritoneal carcinomatosis.* Clin Exp Immunol, 2000. **119**(1): p. 19-27.

123. Collins, A.V., et al., *The interaction properties of costimulatory molecules revisited.* Immunity, 2002. **17**(2): p. 201-10.

124. Lim, T.S., et al., *CD80 and CD86 differentially regulate mechanical interactions of T-cells with antigen-presenting dendritic cells and B-cells.* PLoS One, 2012. **7**(9): p. e45185.

125. Beltrame, M.H., et al., *CD80 and CD86 polymorphisms in populations of various ancestries: 5 new CD80 promoter alleles.* Hum Immunol, 2012. **73**(1): p. 111-7.

126. Gribben, J.G., et al., *CTLA4 mediates antigen-specific apoptosis of human T cells.* Proc Natl Acad Sci U S A, 1995. **92**(3): p. 811-5.

127. Yokosuka, T., et al., *Spatiotemporal basis of CTLA-4 costimulatory molecule-mediated negative regulation of T cell activation.* Immunity, 2010. **33**(3): p. 326-39.

128. Lux, A. and F. Nimmerjahn, *Of mice and men: the need for humanized mouse models to study human IgG activity in vivo.* J Clin Immunol, 2013. **33 Suppl 1**: p. S4-8.

129. Ueda, O., et al., *Novel genetically-humanized mouse model established to evaluate efficacy of therapeutic agents to human interleukin-6 receptor*. Sci Rep, 2013. **3**: p. 1196.

130. Lang, J., et al., *Studies of lymphocyte reconstitution in a humanized mouse model reveal a requirement of T cells for human B cell maturation.* J Immunol, 2013. **190**(5): p. 2090-101.